NATIONAL ADVISORY COMMITTEE FOR AERONAUTICS

TECHNICAL NOTE

No. 1232

EFFECT OF EXHAUST PRESSURE ON THE PERFORMANCE OF AN 18-CYLINDER AIR-COOLED RADIAL ENGINE WITH A VALVE OVERLAP OF 62°

By Leroy V. Humble, Tibor F. Nagey
and David S. Boman

Aircraft Engine Research Laboratory
Cleveland, Ohio

Washington
March 1947

NATIONAL ADVISORY COMMITTEE FOR AERONAUTICS

TECHNICAL NOTE NO. 1232

EFFECT OF EXHAUST PRESSURE ON THE PERFORMANCE OF AN 18-CYLINDER AIR-COOLED RADIAL ENGINE WITH A VALVE OVERLAP OF 62°

By Leroy V. Humble, Tibor F. Nagey
and David S. Boman

SUMMARY

A dynamometer-stand investigation was conducted to determine the effect of exhaust pressure on the performance of an 18-cylinder air-cooled, radial engine equipped with a conventional exhaust collector ring. The investigation covered a range of engine speeds from 1400 to 2600 rpm, inlet-manifold pressures from 30 to 50 inches of mercury absolute, fuel-air ratios of 0.063, 0.069, 0.085, and 0.100, and spark settings of 20° and 35° B.T.C. The exhaust pressure was varied, in general, from approximately 6 inches of mercury absolute to about 20 inches of mercury above the inlet-manifold pressure.

At constant values of engine speed, inlet-manifold pressure, carburetor-air temperature, fuel-air ratio, and cooling-air pressure drop, an increase in exhaust pressure resulted in a decrease in power and charge-air flow and in an increase in inlet-manifold temperature and average cylinder-head temperature. The exhaust-gas temperature reached a peak value at an exhaust pressure of about 0.8 of the inlet-manifold pressure.

Comparison of the results of the present investigation with those previously obtained on a similar engine, which had a smaller nominal valve overlap (40°), showed that the effect of exhaust pressure on engine power and charge-air flow was greater on the engine with 62° valve overlap. For example, at an engine speed of 2000 rpm, an inlet-manifold pressure of 30 inches of mercury absolute, and a fuel-air ratio of 0.085, a change in the ratio of exhaust pressure to inlet-manifold pressure from 0.2 to 1.6 caused a 52-percent decrease in brake horsepower on the engine with 62° valve overlap and a 31-percent decrease on the engine with the 40° valve overlap.

INTRODUCTION

A research program was instituted at the NACA Cleveland laboratory to determine the increase in power and efficiency obtainable by gearing an exhaust-gas turbine and a compressor to the crankshaft of a conventional aircraft engine.

As the first phase of the program, a dynamometer-stand investigation was made on an 18-cylinder, air-cooled, radial engine with a 40° valve overlap to determine the effect of exhaust pressure on engine performance and cooling. The results of this investigation are reported in references 1 and 2. The computed performance of a composite system consisting of this engine with a turbine and a compressor mounted on a common shaft and geared to the crankshaft is reported in reference 3.

During the course of the foregoing investigation, a newer model engine of the same type, which incorporated several changes including an increase in nominal valve overlap from 40° to 62°, became available. Because the change in valve timing was expected to influence the effect of exhaust pressure on engine performance, an investigation similar to that reported in reference 1 was conducted with the newer model engine.

The investigation covered a range of engine speeds, inlet-manifold pressures, and fuel-air ratios. The exhaust pressure was varied over a wide range with various combinations of these variables.

The results are presented in the form of curves that show the effect of exhaust pressure on engine power, charge-air flow, volumetric efficiency, inlet-manifold temperature, cylinder-head temperature, and exhaust-gas temperature. Representative curves taken from reference 1 are included for comparison.

INSTALLATION AND INSTRUMENTATION

The R-2800-57, 18-cylinder, air-cooled, radial engine used for this investigation has a take-off rating of 2100 brake horsepower at 2800 rpm and a normal rating of 1700 brake horsepower at 2600 rpm. Pertinent specifications for this engine and for the R-2800-5 engine (reference 1) are given for comparison:

	R-2800-57 engine	R-2800-5 engine
Bore, inches	5.75	5.75
Stroke, inches	6.00	6.00
Displacement, cubic inches	2804	2804
Compression ratio	6.75	6.65
Propeller-reduction-gear ratio	0.45:1	0.5:1
Valve overlap, degrees	62	40
Spark setting, degrees B.T.C.:		
Cruising advance	35	25
Normal advance	20	25
Blower-gear ratio:		
Low	7.29:1	7.6:1
High	None	9.45:1
Impeller diameter, inches	11.5	11.0

The engine was equipped with an automatic two-position spark-advance unit, which was altered so that it could be locked in either of the two positions (20° or 35° B.T.C.).

A photograph and a sketch of the setup are shown in figures 1 and 2, respectively. The installation and instrumentation was essentially the same as described in reference 1.

The exhaust collector ring was the same as that used in reference 1 except that the original expansion joints were replaced by a sleeve-type expansion joint enclosed in a gastight bellows. The collector ring was built in halves and connected to the laboratory altitude exhaust system through a Y-shaped section of pipe and a large diameter 90° miter elbow. The engine exhaust pressure was measured by a static-pressure tap located where the exhaust pipe was connected to the 90° elbow.

Exhaust-gas temperatures were measured, as in reference 1, approximately 18 inches downstream of the junction of the Y-shaped section with three quadruple-shielded chromel-alumel thermocouples immersed to about 0.3 of the pipe diameter and spaced 120°.

The cooling-air total pressure in front of the engine was measured ahead of cylinders 4, 10, and 16. Two shrouded total-pressure tubes were mounted on supports in front of each of the three cylinders: one at the same radial distance as the middle circumferential head fin and one at the same radial distance as the center of the cylinder barrel. The cooling-air inlet temperature was measured by three thermocouples wired in parallel and mounted on the total-pressure-tube supports.

In reference 1, static pressure behind the heads was measured with a tube on each rear-row cylinder and the static pressure behind the barrels was measured with three static-pressure tubes mounted on supports behind the rear-row cylinders. For the present investigation, the static pressure behind the heads was measured with open-end tubes placed in the sheltered region behind the baffle curl on the inlet side of cylinders 1, 5, 9, and 15 at the same radial distance as the cylinder-head total-pressure tubes. The static pressure behind the barrels was similarly obtained on the same cylinders with tubes located at the same radial distance as the cylinder-barrel total-pressure tubes.

Cylinder-head temperatures were measured on all cylinders with bayonet-type thermocouples located in wells at the rear center of the cylinder heads. This thermocouple replaced the rear spark-plug boss and gasket thermocouples used in reference 1. Barrel temperatures were measured on all cylinders with thermocouples that were peened into the muff at the rear center of the barrel.

The total pressure at the carburetor top deck was taken as the carburetor-inlet pressure and the carburetor-air temperature was taken as the value obtained with six thermocouples connected in parallel and located in the air stream about 5 inches above the carburetor top deck. The inlet-manifold (blower-rim) pressure was measured at a manifold-pressure-gage connection in the blower housing. The inlet-manifold (mixture) temperature in the inlet pipes was obtained by averaging the temperatures measured with an unshielded thermocouple placed in the center of each inlet pipe approximately 4 inches from the port.

PROCEDURE

The investigation covered a range of engine speeds from 1400 to 2600 rpm, inlet-manifold pressures from 30 to 50 inches of mercury absolute, and fuel-air ratios of 0.063, 0.069, 0.085, and 0.100. Most of the investigation was made with the normal spark setting of 20° B.T.C.; some data were obtained, however, at low power with the cruising setting of 35° B.T.C. With each of the foregoing variables held constant, the exhaust pressure was varied from approximately 6 inches of mercury absolute to about 20 inches of mercury above the inlet-manifold pressure, except during high manifold-pressure operation where instrument limitations occurred and in a few other cases when engine operation became unstable or incipient detonation occurred.

For each series of runs, the cooling-air pressure drop was so adjusted that the maximum cylinder-barrel temperature was between 280° and 300° F (the corresponding maximum head temperature was between 320° and 375° F) with the exhaust pressure at approximately 28 inches of mercury absolute. The cooling-air pressure drop was then maintained constant at this value while the exhaust pressure was varied. Sufficient time was allowed at each value of exhaust pressure for the cylinder temperatures to reach equilibrium. The oil-in temperature was maintained at 160° ±10° F.

In most cases the engine charge air was taken into the induction system directly from the atmosphere; in some cases, it was obtained from the laboratory high-pressure air supply. The charge air was furnished to the carburetor at a pressure sufficient to give the desired inlet-manifold pressure with full-open engine throttle, the carburetor-inlet pressure being controlled by means of a butterfly valve located in the charge-air pipe between the air-measuring orifice and the carburetor. All engine data were obtained with the engine throttle in full-open position.

RESULTS AND DISCUSSION

The data are presented in a manner similar to that of reference 1; representative curves from reference 1 are included for comparison.

Effect of exhaust pressure on indicated power. - The dimensionless quantity ϕ (ratio of engine indicated mean effective pressure to engine inlet-manifold pressure) is used as a measure of indicated power (reference 4).

The indicated mean effective pressure (and hence ϕ) is defined to include the contributions of all four strokes of the cycle; ϕ was corrected to a constant inlet-manifold temperature of 660° R on the assumption that indicated power varied inversely as the absolute inlet-manifold temperature. The variation of the ratio ϕ with the ratio of engine exhaust pressure to inlet-manifold pressure p_e/p_m for the various inlet-manifold pressures is shown in figure 3 for constant values of engine speed, fuel-air ratio, and spark setting. As in reference 1, the plots are independent of inlet-manifold pressure for the range covered. The effect of speed on ϕ is small within the range investigated for speeds of 2200 rpm and above.

Faired curves (taken from reference 1) showing the variation of ϕ with p_e/p_m for the engine with 40° valve overlap at a fuel-air ratio of 0.085 are included in figure 3(b) for comparison. Although the curves for the two engines are for slightly different spark settings, the differences between them may be considered as illustrative of the effect of the different valve overlaps. For example, at an engine speed of 2000 rpm, increasing p_e/p_m from 0.2 to 1.6 results in a decrease in ϕ of 42 and 25 percent for the 62° and 40° valve overlaps, respectively.

Effect of exhaust pressure on brake horsepower. - The variation of brake horsepower with p_e/p_m for various engine speeds, inlet-manifold pressures, fuel-air ratios, and for two spark settings is shown in figure 4. During the investigation, the carburetor-air temperature varied slightly from 550° R and the brake horsepower was corrected to 550° R on the assumption that the power varied inversely as the square root of the absolute carburetor-air temperature. The inlet-manifold temperature, as shown in a later section, increases with exhaust pressure for constant carburetor-air temperature. The brake horsepower shown in figure 4, which was corrected to a constant carburetor-air temperature, thus includes the effect of the varying inlet-manifold temperature; whereas the curves of ϕ in figure 3, which were corrected to constant inlet-manifold temperature, do not.

The brake horsepower was measured with the engine throttle in the full-open position, the carburetor being supplied with air at a pressure sufficient to give the desired pressure at the inlet manifold. The variation of the ratio of inlet-manifold pressure to full-throttle carburetor-inlet pressure p_m/p_c with engine speed is shown in figure 5. This faired curve, which is plotted for a carburetor-air temperature of 550° R, is included to facilitate the determination of p_c for the various operating conditions. The curve is accurate to about ±1.5 percent for values of p_e/p_m near 1.0 and to about ±2.5 percent over the range of p_e/p_m covered.

Faired curves of brake horsepower against p_e/p_m, obtained from figure 4, are shown in figure 6 with similar curves (blower gear ratio, 7.6:1) from reference 1 for several engine speeds at a fuel-air ratio of 0.085 and inlet-manifold pressures of 30 and 40 inches of mercury absolute. The effect of valve overlap is again evident. At an engine speed of 2000 rpm, and an inlet-manifold pressure of 30 inches of mercury absolute, a change in p_e/p_m from 0.2 to 1.6 causes 52- and 31-percent decreases in power for the 62° and 40° valve overlaps, respectively.

The effect of exhaust pressure on engine brake horsepower can be generalized by use of the dimensionless quantity α, defined as the ratio of the brake horsepower at any value of p_e/p_m to the brake horsepower at $p_e/p_m = 1.0$ for the same altitude, engine speed, inlet-manifold pressure, fuel-air ratio, and spark setting. The variation of α with p_e/p_m for constant engine speeds is shown in figure 7. Each curve represents the best possible fairing for all the data obtained at that engine speed.

Effect of exhaust pressure on charge-air flow and volumetric efficiency. - The variation of charge-air flow W_c with p_e/p_m for various engine speeds, inlet-manifold pressures, fuel-air ratios, and for two spark settings is shown in figure 8. The charge-air flow was corrected to a carburetor-air temperature of 550° R by the same method as the brake horsepower. The figure shows that charge-air flow decreases with increasing p_e/p_m in much the same way as power.

Faired curves of charge-air flow against p_e/p_m obtained from figure 8 are shown in figure 9 with similar curves (blower gear ratio, 7.6:1) from reference 1 for several engine speeds at a fuel-air ratio of 0.085 and inlet-manifold pressures of 30 and 40 inches of mercury absolute. In general, the engine with 62° valve overlap had a greater breathing capacity than the engine with 40° valve overlap when p_e/p_m was less than 1.0 and a smaller capacity when p_e/p_m was greater than 1.0.

The volumetric efficiency (defined as the ratio of the volume of charge air taken into the engine per cycle at inlet-manifold pressure and temperature to the displacement volume of the engine) is plotted against p_e/p_m for constant engine speeds in figure 10; curves from reference 1 are included for comparison. The data obtained with the engine with 62° overlap over the range of exhaust pressures at the various inlet-manifold pressures, fuel-air ratios, and at two spark settings are included in figure 10 and good correlation of the data is observed.

From figures 5 and 8 the auxiliary supercharger power required to supply the charge air to the carburetor can be computed for any altitude and engine condition. This auxiliary supercharger power must be subtracted from the measured brake horsepower to obtain the actual brake horsepower because in this investigation the carburetor air was supplied by the laboratory air system at the pressure necessary to give the desired inlet-manifold pressure.

Variation of power with charge-air flow. - The variation of indicated horsepower minus pumping horsepower (ihp - php), which represents the work of only the compression and expansion strokes of the cycle, with charge-air flow W_c is shown in figure 11. Separate plots are shown for each fuel-air ratio and spark setting, and each plot is keyed according to engine speed. The data obtained over the range of exhaust pressures at each inlet-manifold prossure are included in the points shown for each engine speed. Power and air flow were corrected to a constant inlet-manifold temperature of 660° R.

The correlation of the data is, in general, satisfactory. The scatter that occurs is probably mainly due to blow-through of charge during the valve overlap period at low exhaust pressures, to systematic errors in the estimation of pumping power, which was based on a square indicator card, and to small changes in combustion and cycle efficiency.

Effect of exhaust pressure on inlet-manifold temperature. - The present investigation showed that, with constant carburetor-air temperature, engine speed, inlet-manifold pressure, and fuel-air ratio, the inlet-manifold temperature tended to increase as the engine exhaust pressure was increased. This increase is illustrated in figure 12 where $T_m - T_c$ (inlet-manifold temperature minus carburetor-air temperature) is plotted against p_e/p_m for constant engine speeds and fuel-air ratios at a carburetor-air temperature of approximately 550° R. The plots are independent of inlet-manifold pressure and spark setting. The increase of $T_m - T_c$ with p_e/p_m is considerably more pronounced at low than at high engine speeds, and when the exhaust pressure is greater than about 0.8 of the inlet-manifold pressure.

Exhaust-gas temperature. - Exhaust-gas temperature, as measured in the unlagged exhaust collector, is plotted against p_e/p_m for the various engine operating conditions in figure 13. The measured temperature increased as engine speed and inlet-manifold pressure increased and as the fuel-air ratio decreased from 0.100 to 0.069; the temperature stayed substantially constant as the fuel-air ratio was further decreased to 0.063. A change in spark setting from 20° to 35° B.T.C. resulted in a decrease in exhaust-gas temperature for otherwise constant conditions, as would be expected because of the improvement in the thermal efficiency of the engine. The temperature reaches a peak value in the region of p_e/p_m near 0.8. Unpublished data obtained on the engine of reference 1 indicated that, with the collector well lagged, the exhaust-gas temperatures were about 250° F higher than with the unlagged collector.

Effect of exhaust pressure on cylinder-head temperature. - The variation of cylinder-head temperature with exhaust pressure is shown in figure 14 by plotting the quantity $(T_h - T_a)/(T_h - T_a)_1$ against p_e/p_m for constant inlet-manifold pressures, engine speeds, and fuel-air ratios. The cooling-air pressure drop across the cylinder heads was very nearly constant for each set of variable exhaust-pressure runs and the average values are listed in the figure. The quantity $(T_h - T_a)$ is the difference between the average cylinder-head temperature and the cooling-air inlet temperature: $(T_h - T_a)_1$ is the corresponding value at $p_e/p_m = 1.0$. The quantity $(T_h - T_a)/(T_h - T_a)_1$ increases with increasing p_e/p_m despite the consistent decrease in power level shown in figure 3.

SUMMARY OF RESULTS

The results of a dynamometer-stand investigation conducted with an engine with 62° valve overlap (R-2800-57 (C-series)) over a range of engine speeds from 1400 to 2600 rpm, inlet-manifold pressures from 30 to 50 inches of mercury absolute, exhaust pressures from about 6 inches of mercury absolute to approximately 20 inches of mercury above the inlet-manifold pressure, fuel-air ratios of 0.063, 0.069, 0.085, and 0.100, and spark settings of 20° and 35° B.T.C. may be summarized as follows:

1. At constant values of engine speed, inlet-manifold pressure, carburetor-air temperature, fuel-air ratio, and cooling-air pressure drop:

(a) Engine power and charge-air flow decreased as the exhaust pressure increased.

(b) Inlet-manifold temperature increased with exhaust pressure. The effect was more pronounced at low than at high engine speeds and at exhaust pressures greater than about 0.8 of the inlet-manifold pressure.

(c) Average cylinder-head temperature increased with exhaust pressure.

(d) Exhaust-gas temperature reached a peak value at an exhaust pressure of about 0.8 of the inlet-manifold pressure. In general, the exhaust-gas temperature increased as engine speed and inlet-manifold pressure increased and as the fuel-air ratio decreased from 0.100 to 0.069; it stayed substantially constant as the fuel-air ratio was further reduced to 0.063.

2. The effect of exhaust pressure on engine power and charge-air flow was greater on the engine with 62° valve overlap than on a similar engine with 40° valve overlap.

Aircraft Engine Research Laboratory,
National Advisory Committee for Aeronautics,
Cleveland, Ohio, January 2, 1947.

REFERENCES

1. Boman, David S., Nagey, Tibor F., and Doyle, Ronald B.: Effect of Exhaust Pressure on the Performance of an 18-Cylinder Air-Cooled Radial Engine with a Valve Overlap of 40°. NACA TN No. 1220, 1947.

2. Valerino, Michael F., Kaufman, Samuel J., and Hughes, Richard F.: Effect of Exhaust Pressure on the Cooling Characteristics of an Air-Cooled Engine. NACA TN No. 1221, 1947.

3. Hannum, Richard W., and Zimmerman, Richard H.: Calculations of the Economy of an 18-Cylinder Radial Aircraft Engine with an Exhaust-Gas Turbine Geared to the Crankshaft at Cruising Speed. NACA ARR No. E5K28, 1945.

4. Pinkel, Benjamin: Effect of Exhaust Back Pressure on Engine Power. NACA CB No. 3F17, 1943.

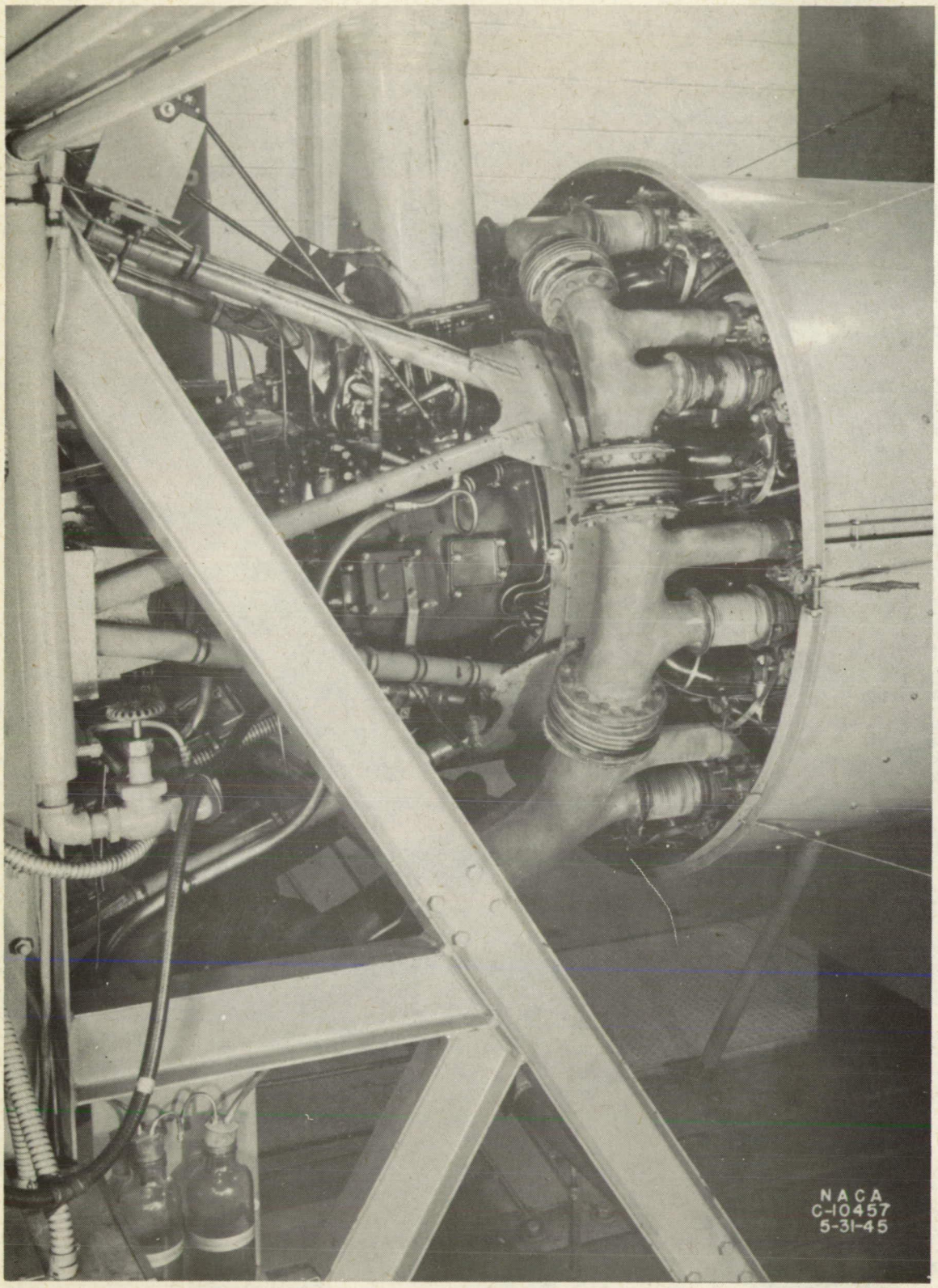

Figure 1. - Dynamometer stand setup for 18-cylinder, air-cooled, radial engine with 62° valve overlap.

NATIONAL ADVISORY
COMMITTEE FOR AERONAUTICS

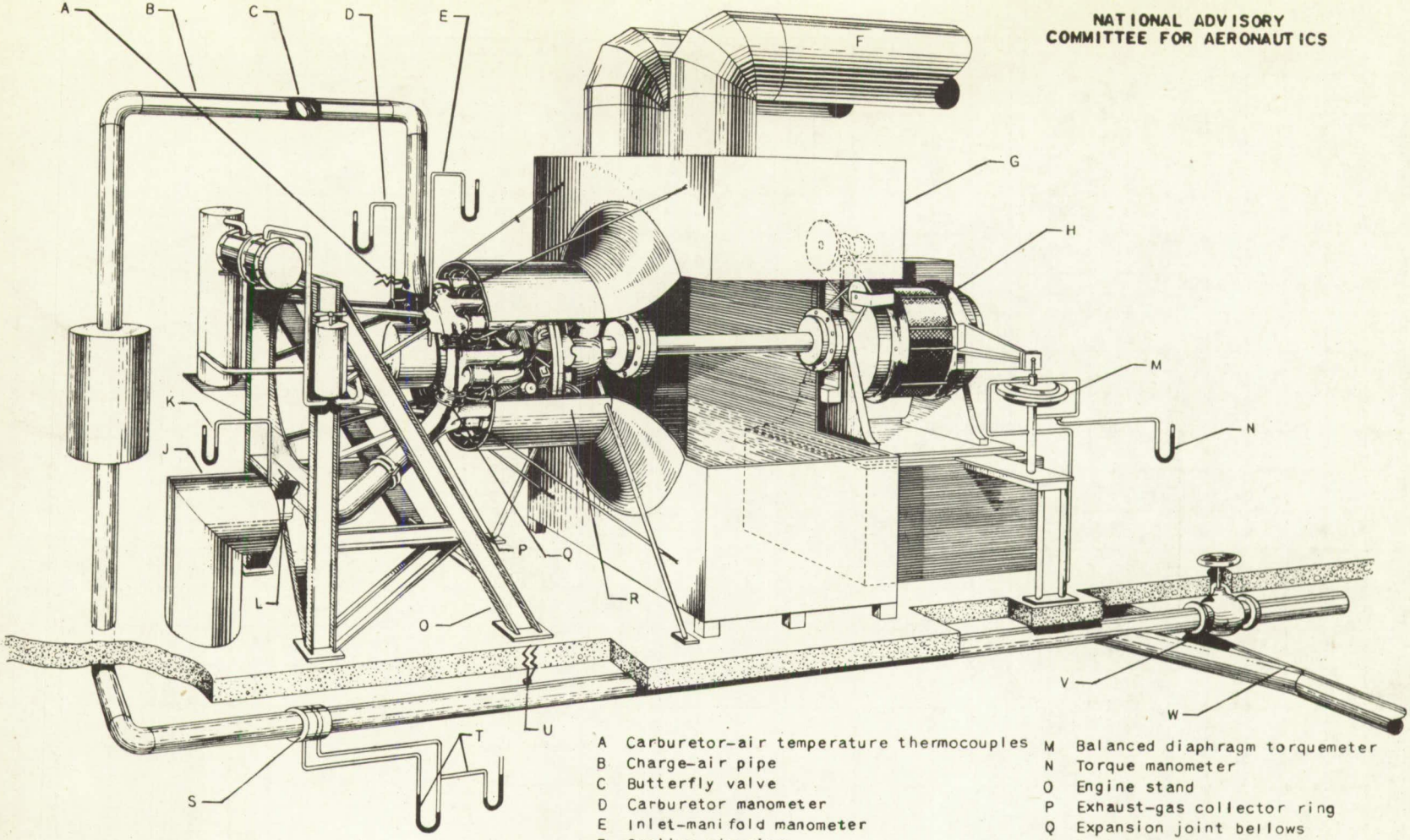

A	Carburetor-air temperature thermocouples	M	Balanced diaphragm torquemeter
B	Charge-air pipe	N	Torque manometer
C	Butterfly valve	O	Engine stand
D	Carburetor manometer	P	Exhaust-gas collector ring
E	Inlet-manifold manometer	Q	Expansion joint bellows
F	Cooling-air pipe	R	Engine cowling
G	Cooling-air box	S	Charge-air orifice
H	Dynamometer	T	Charge-air orifice manometers
J	Elbow section of exhaust ducting	U	Charge-air orifice thermocouples
K	Exhaust manometer	V	Charge-air bleed valve
L	Exhaust-gas thermocouples	W	Laboratory high-pressure air pipe

Figure 2. - Schematic sketch of setup.

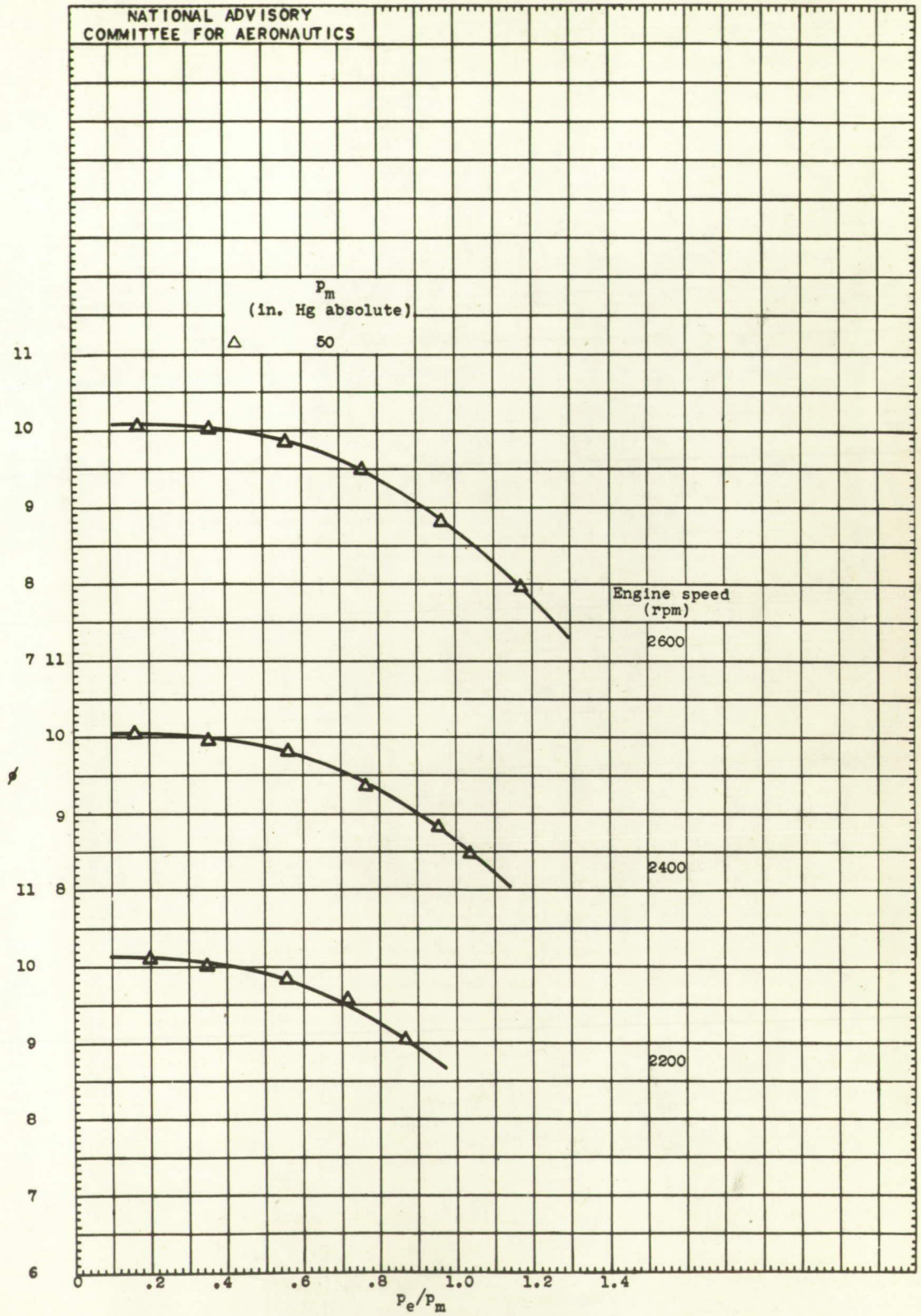

(a) Fuel-air ratio, 0.100; spark setting, 20° B.T.C.

Figure 3. - Variation of ϕ with p_e/p_m. Values of ϕ corrected to constant inlet-manifold temperature of 660° R.

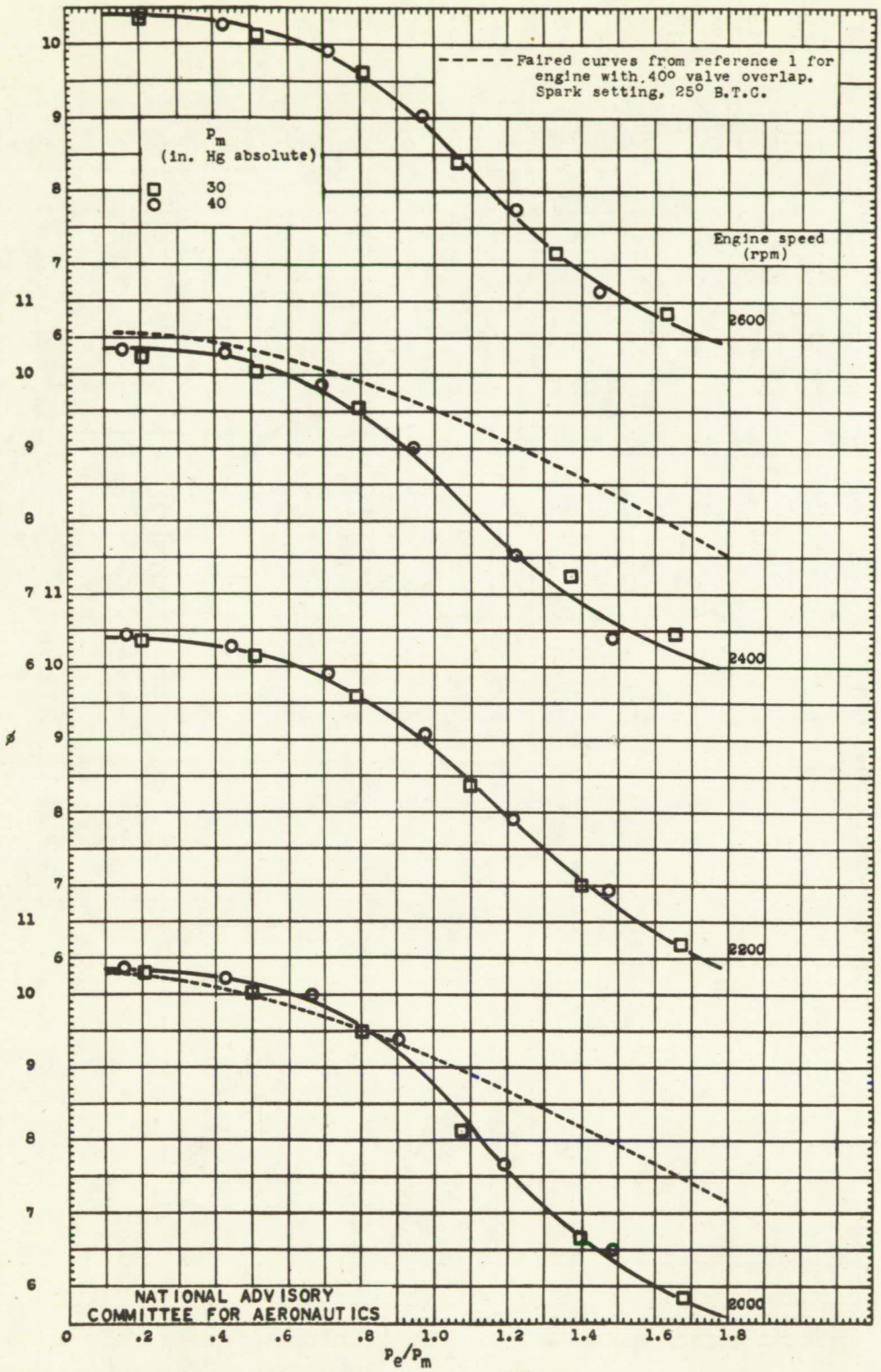

(b) Fuel-air ratio, 0.085; spark setting, 20° B.T.C.

Figure 3. - Continued. Variation of ϕ with p_e/p_m. Values of ϕ corrected to constant inlet-manifold temperature of 660° R.

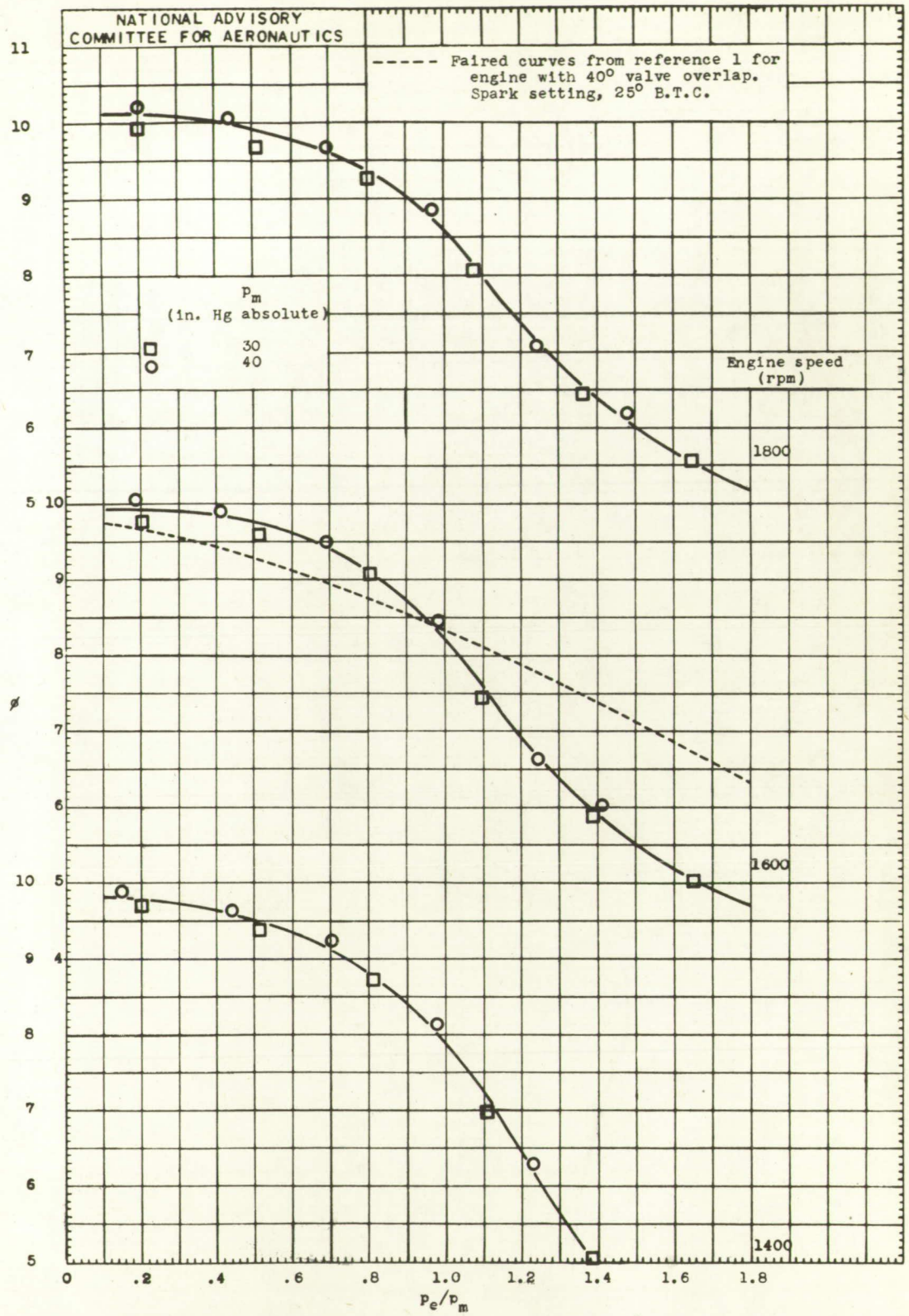

(b) Concluded. Fuel-air ratio, 0.085; spark setting 20° B.T.C.

Figure 3. - Continued. Variation of ø with p_e/p_m. Values of ø corrected to constant inlet-manifold temperature of 660° R.

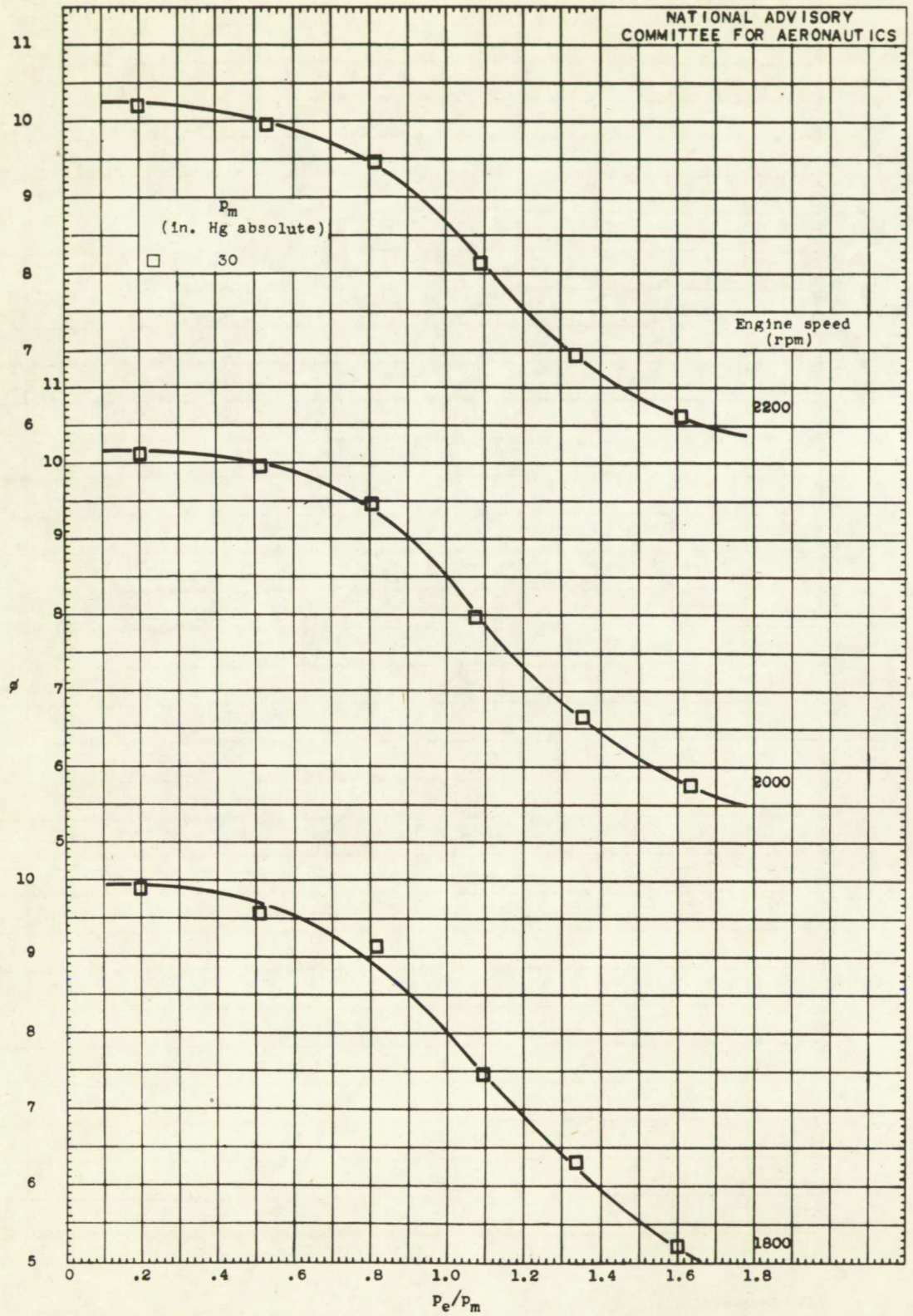

(c) Fuel-air ratio, 0.069; spark setting, 20° B.T.C.

Figure 3. - Continued. Variation of ø with p_e/p_m. Values of ø corrected to constant inlet-manifold temperature of 660° R.

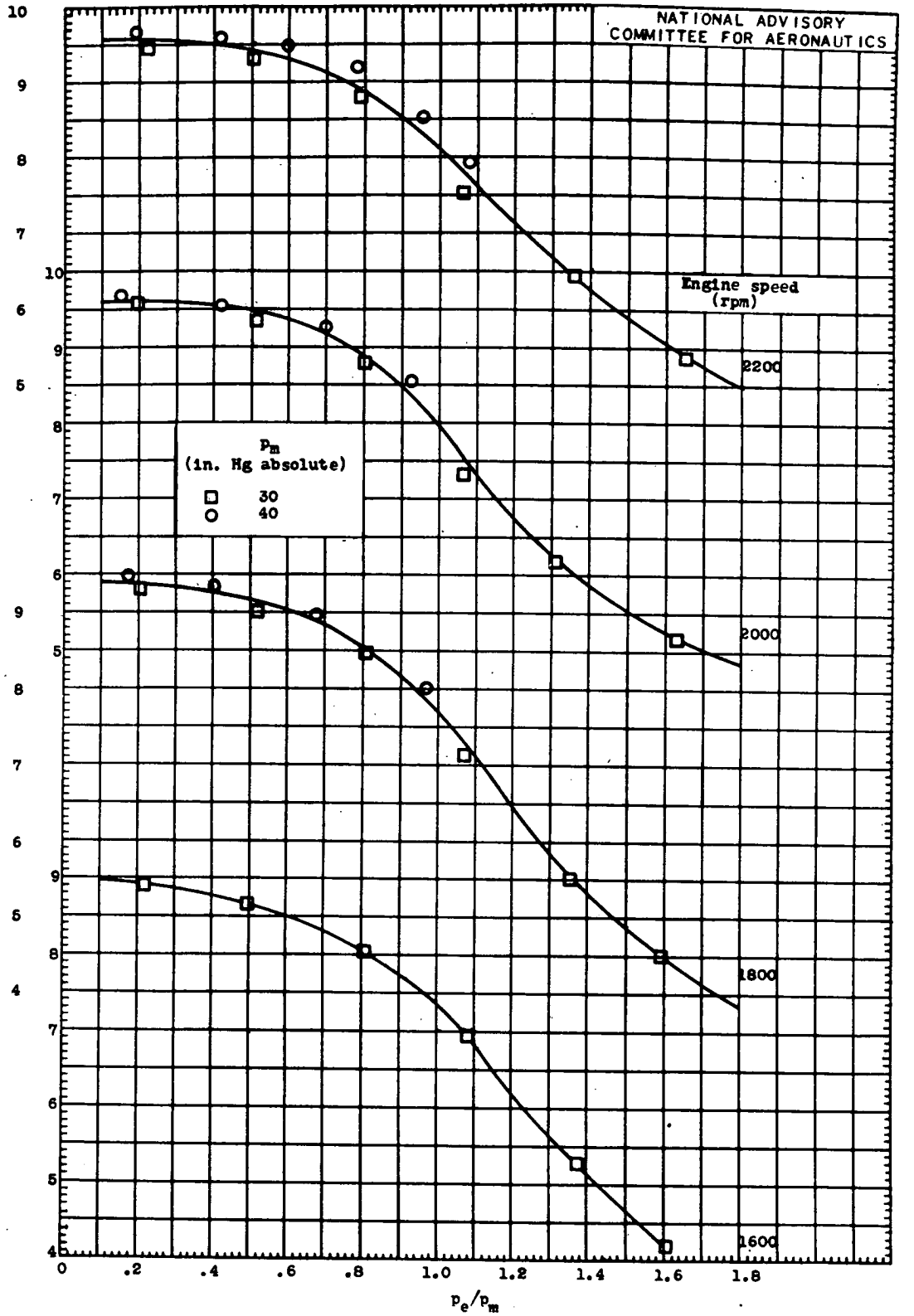

(d) Fuel-air ratio, 0.063; spark setting, 20° B.T.C.

Figure 3. - Continued. Variation of ϕ with p_e/p_m. Values of ϕ corrected to constant inlet-manifold temperature of 660° R.

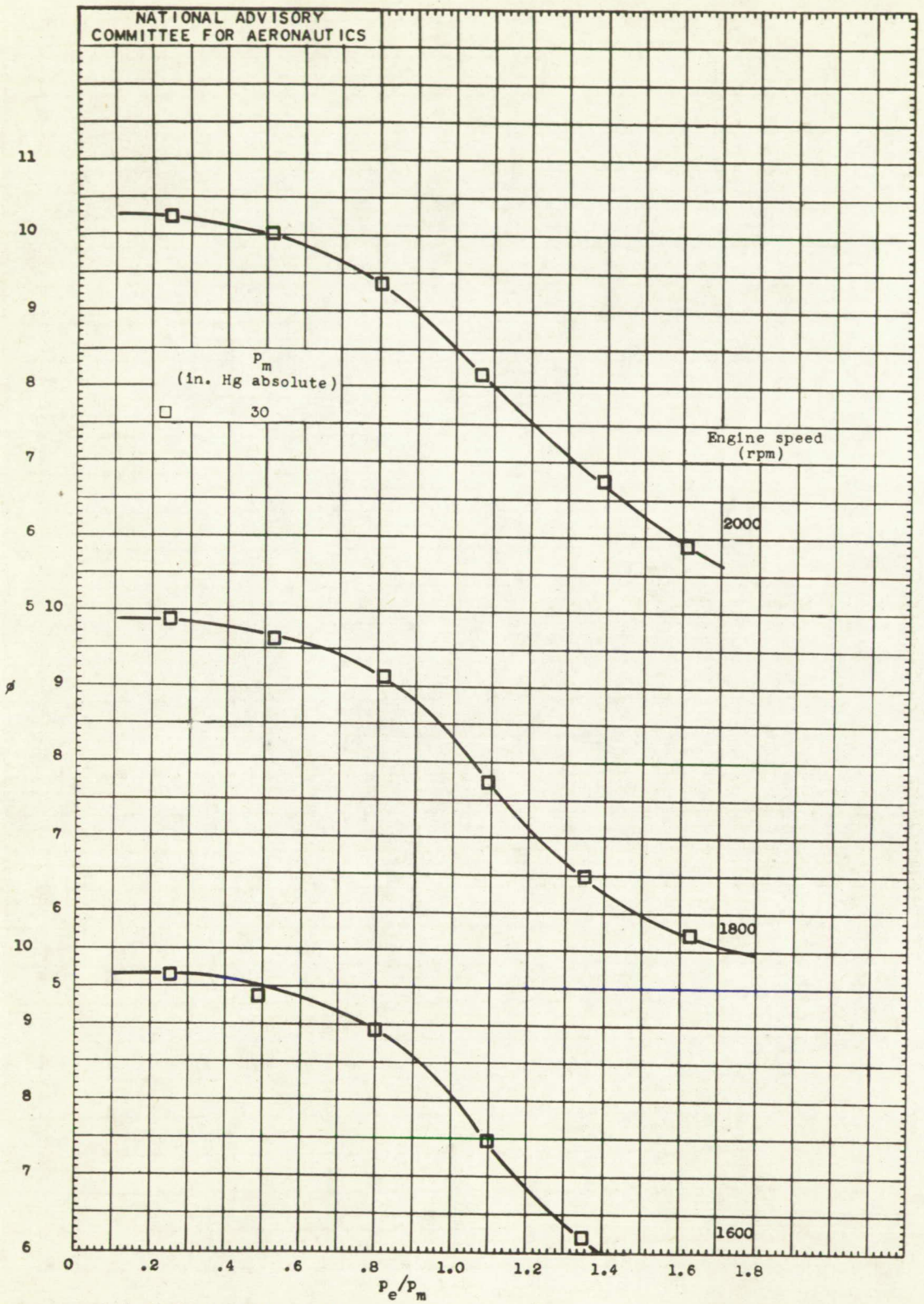

(e) **Fuel-air ratio, 0.063; spark setting, 35° B.T.C.**

Figure 3. - Concluded. Variation of ø with p_e/p_m. Values of ø corrected to constant inlet-manifold temperature of 660° R.

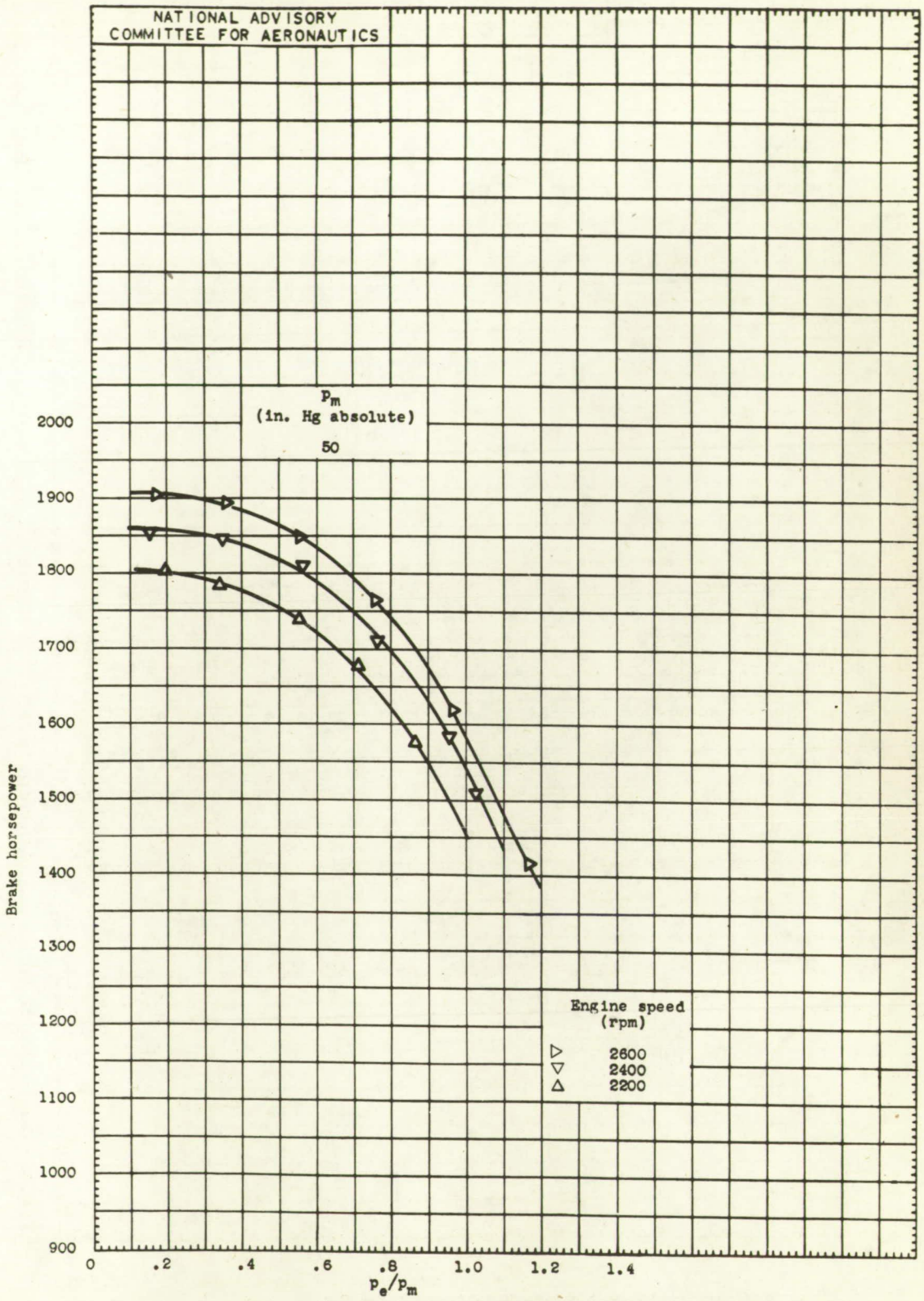

(a) Fuel-air ratio, 0.100; spark setting, 20° B.T.C.

Figure 4. - Variation of brake horsepower with p_e/p_m. Brake horsepower corrected to constant carburetor-air temperature of 550° R.

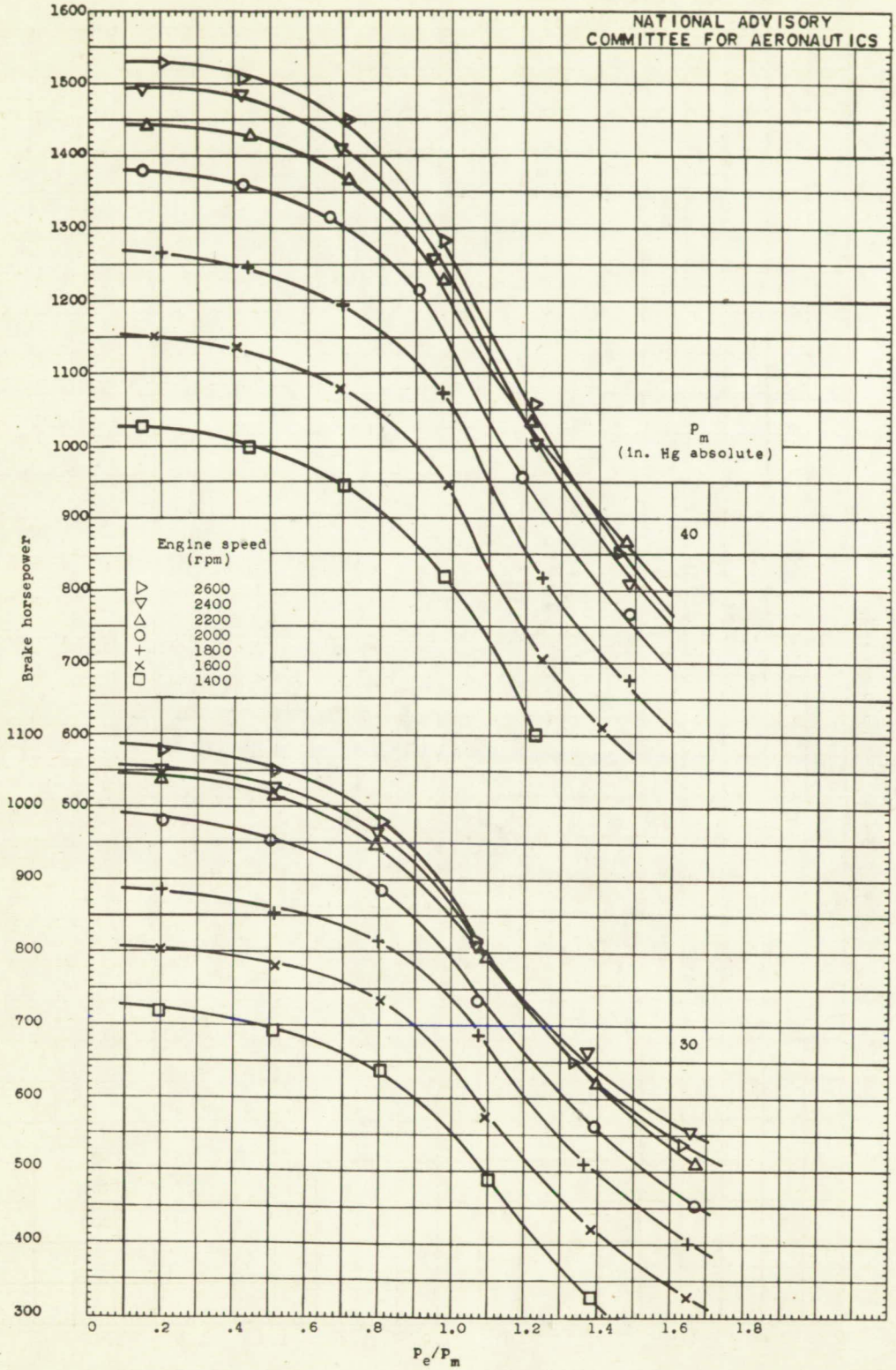

(b) Fuel-air ratio, 0.085; spark setting, 20° B.T.C.

Figure 4. - Continued. Variation of brake horsepower with p_e/p_m. Brake horsepower corrected to constant carburetor-air temperature of 550° R.

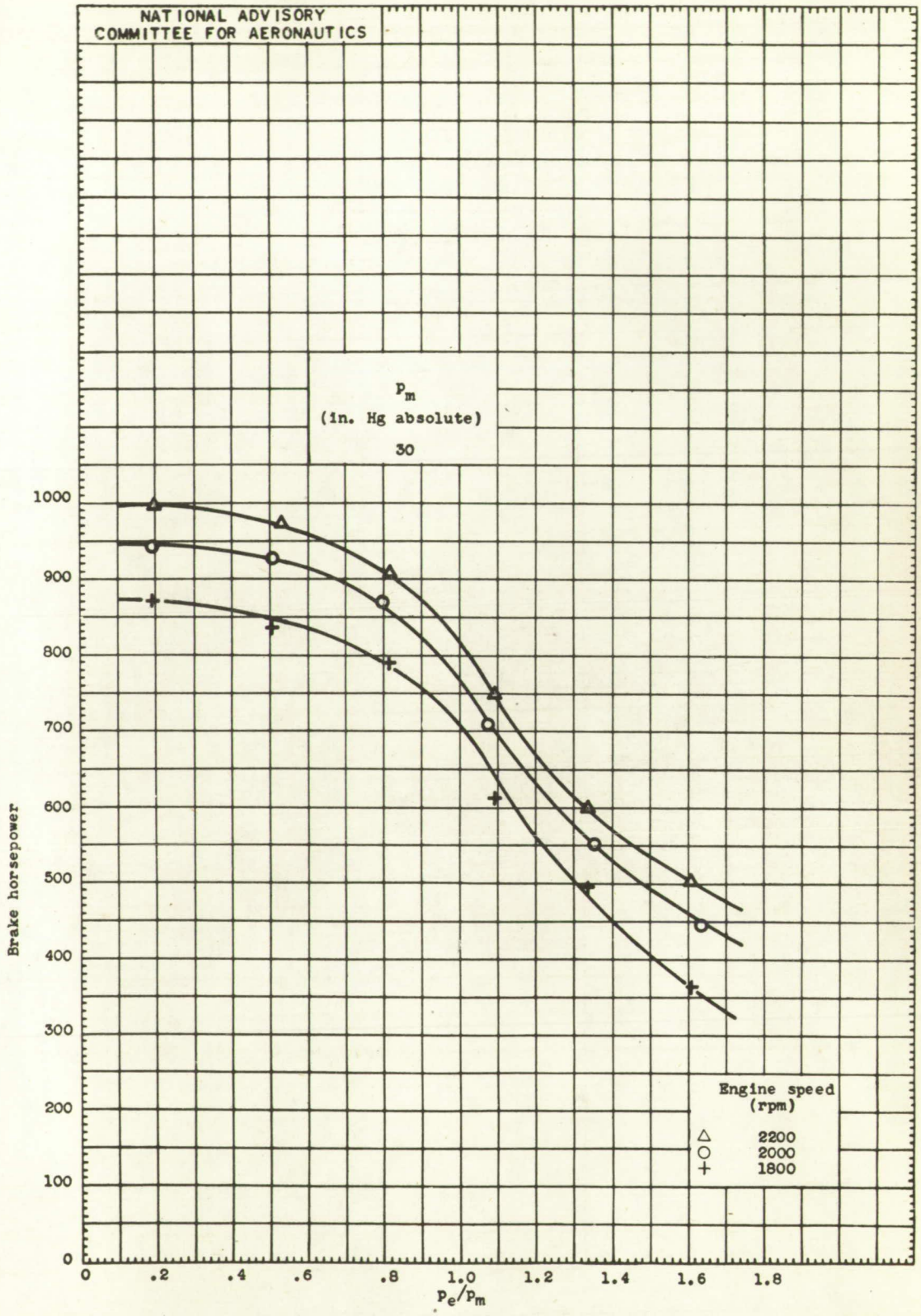

(c) Fuel-air ratio, 0.069; spark setting, 20° B.T.C.

Figure 4. - Continued. Variation of brake horsepower with p_e/p_m. Brake horsepower corrected to constant carburetor-air temperature of 550° R.

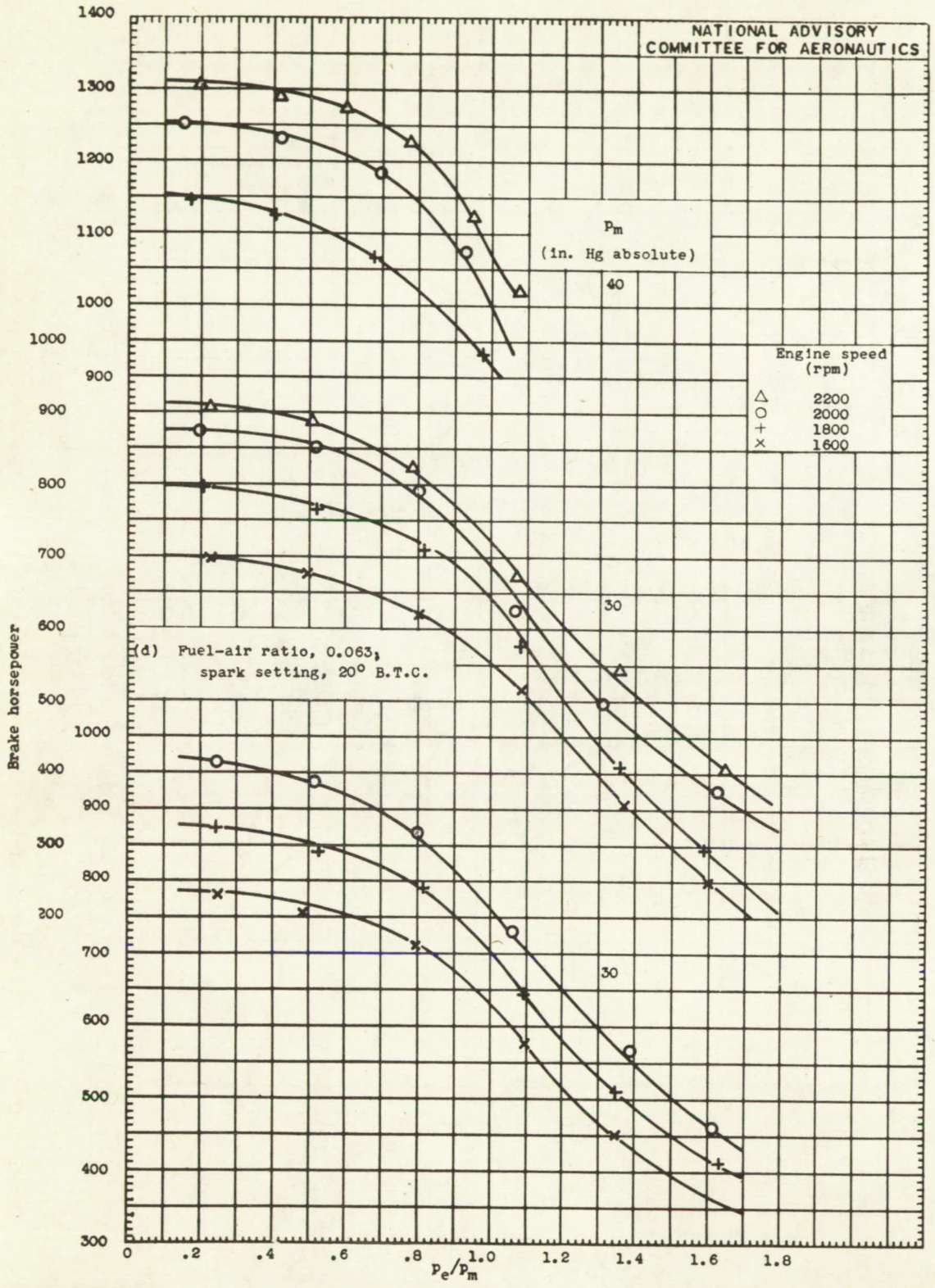

(e) Fuel-air ratio, 0.063; spark setting, 35° B.T.C.

Figure 4. - Concluded. Variation of brake horsepower with p_e/p_m. Brake horsepower corrected to constant carburetor-air temperature of 550° R.

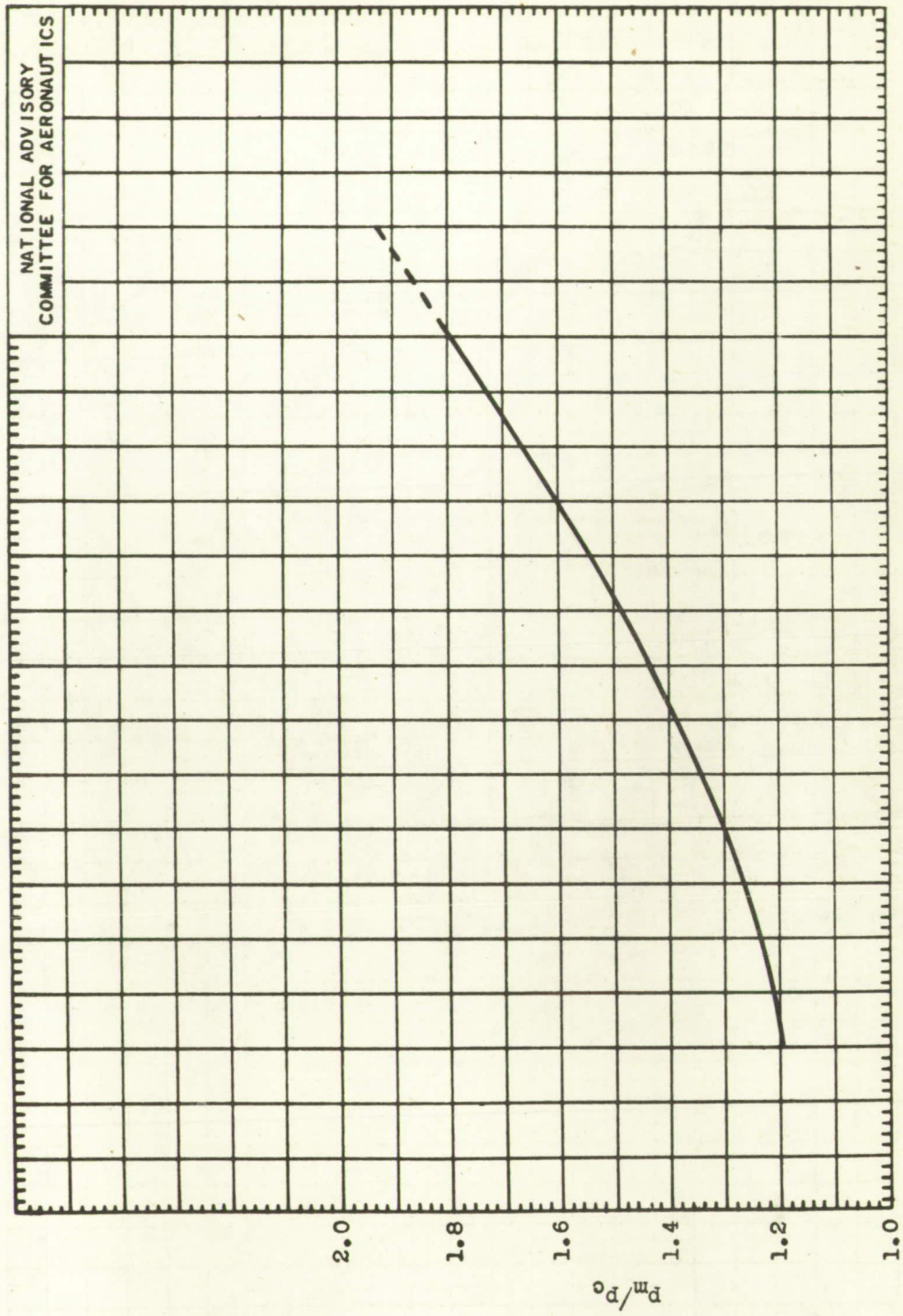

Figure 5. - Variation of ratio of inlet-manifold pressure to full-open throttle carburetor-inlet pressure p_m/p_c with engine speed. Carburetor-air temperature, 550° R.

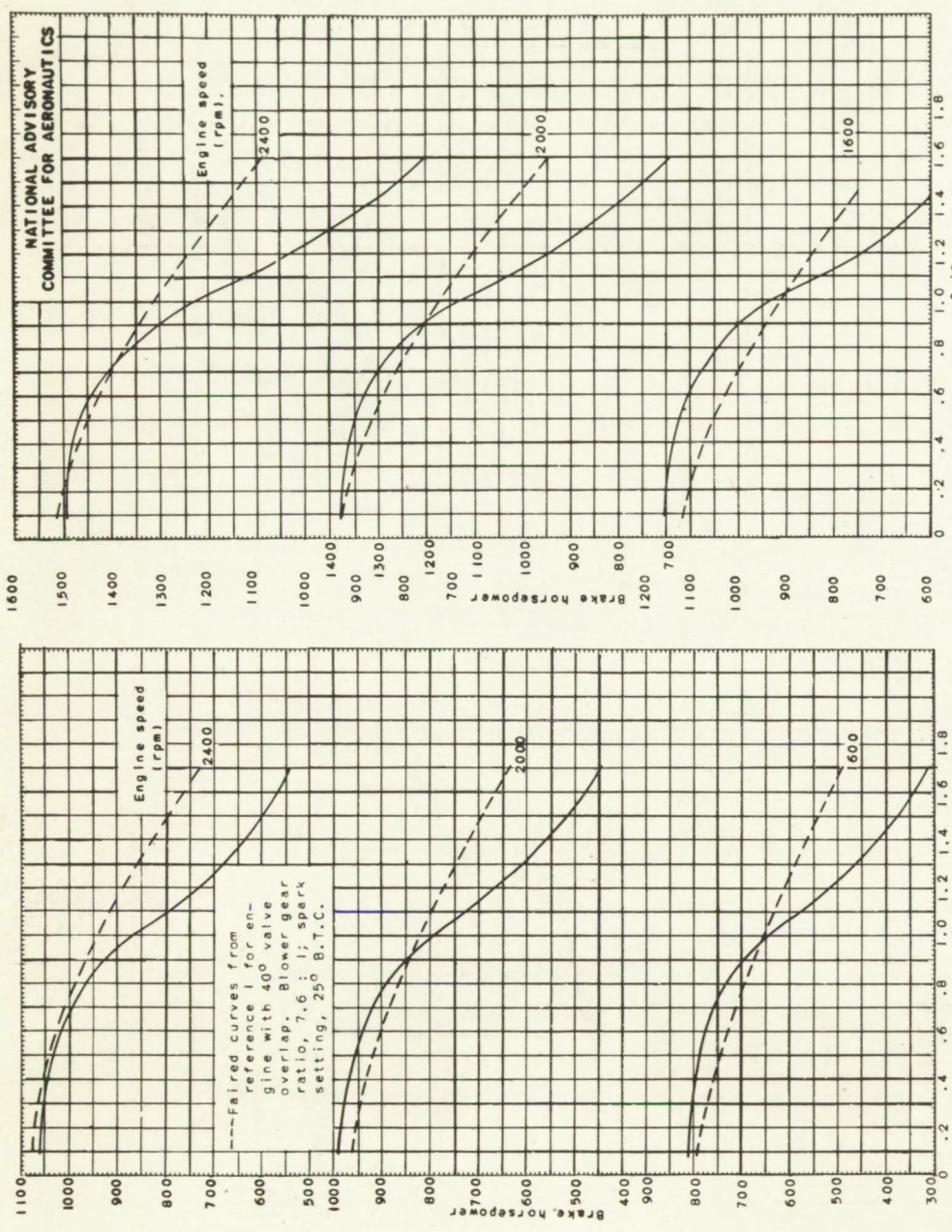

Figure 6. - Faired curves of brake horsepower as taken from figure 4 plotted with faired curves of brake horsepower taken from reference 1. Brake horsepower corrected to constant carburetor-air temperature of 550° R; fuel-air ratio, 0.085.

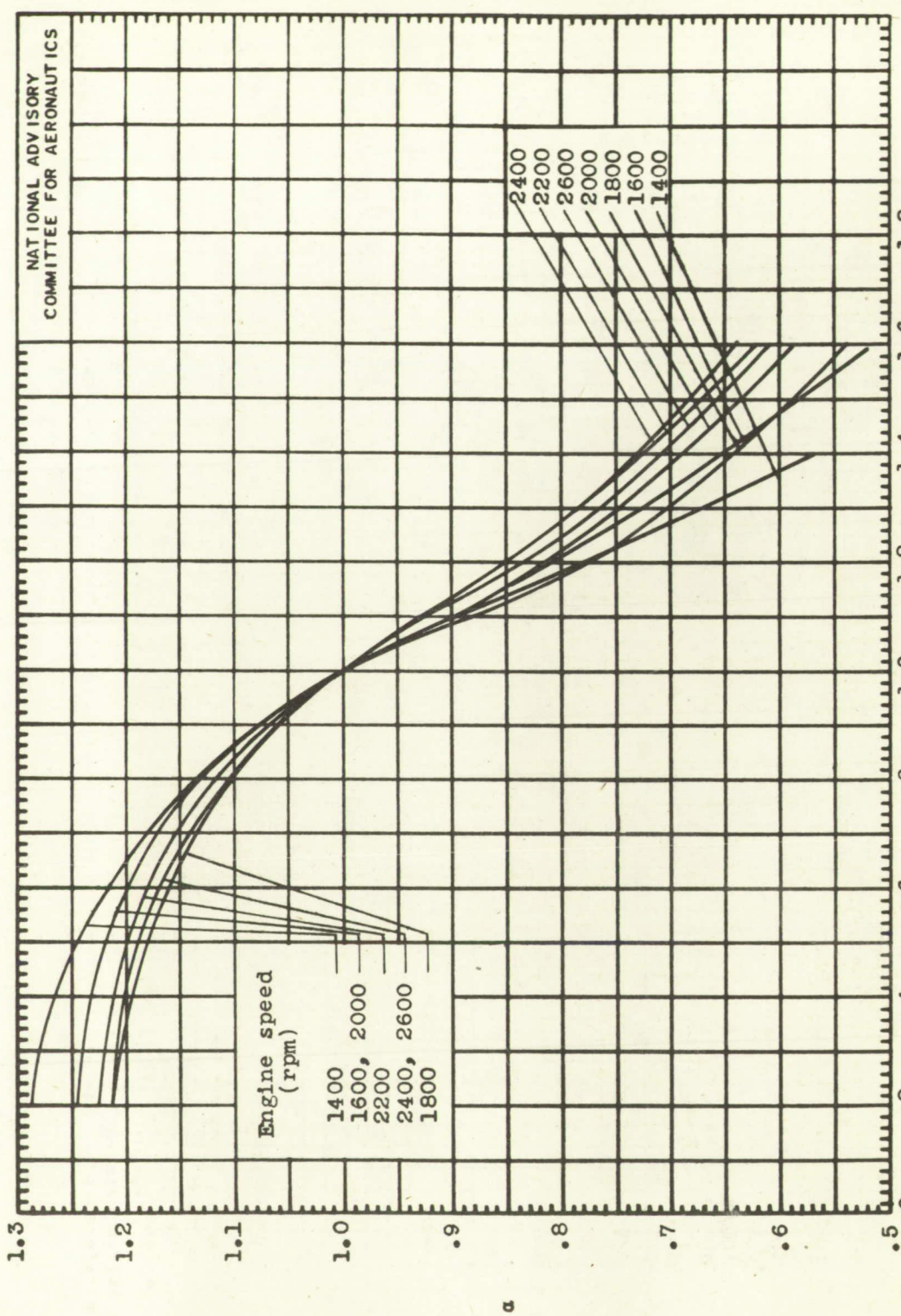

Figure 7. - Variation of α with p_e/p_m for various engine speeds.

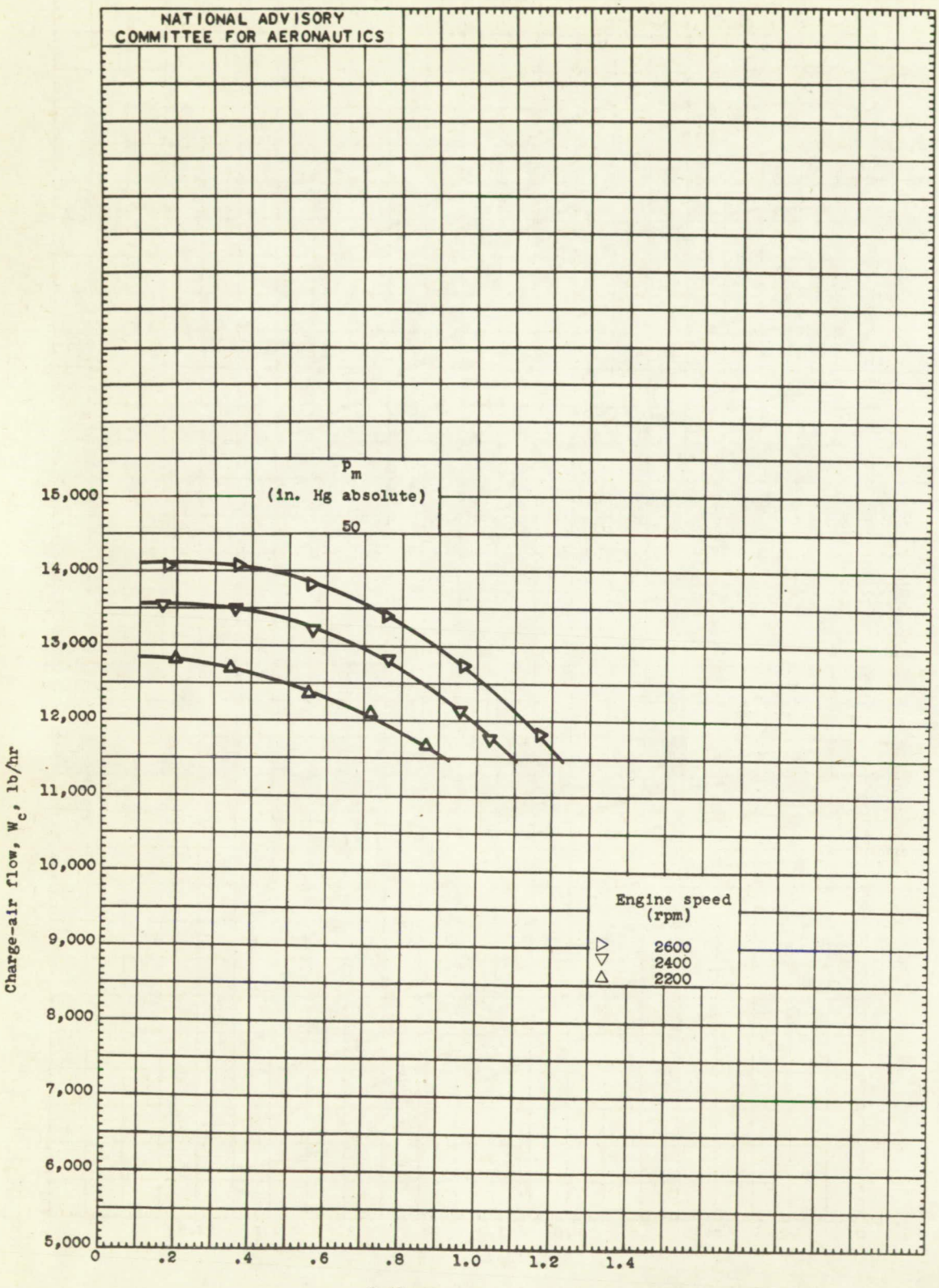

(a) Fuel-air ratio, 0.100; spark setting, 20° B.T.C.

Figure 8. - Variation of charge-air flow W_c with p_e/p_m. Charge-air flow corrected to constant carburetor-air temperature of 550° R.

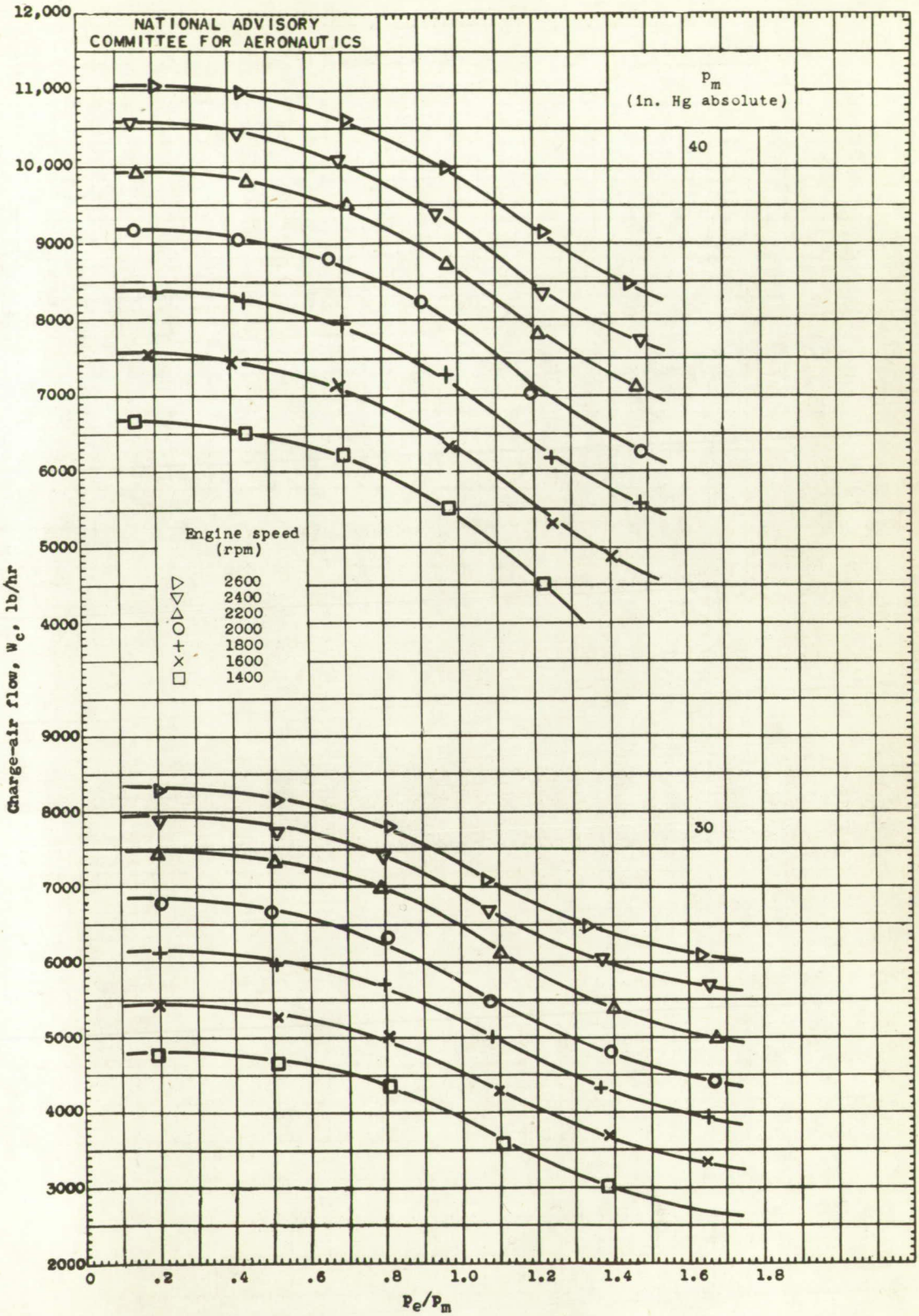

(b) Fuel-air ratio, 0.085; spark setting, 20° B.T.C.

Figure 8. - Continued. Variation of charge-air flow W_c with p_e/p_m. Charge-air flow corrected to constant carburetor-air temperature of 550° R.

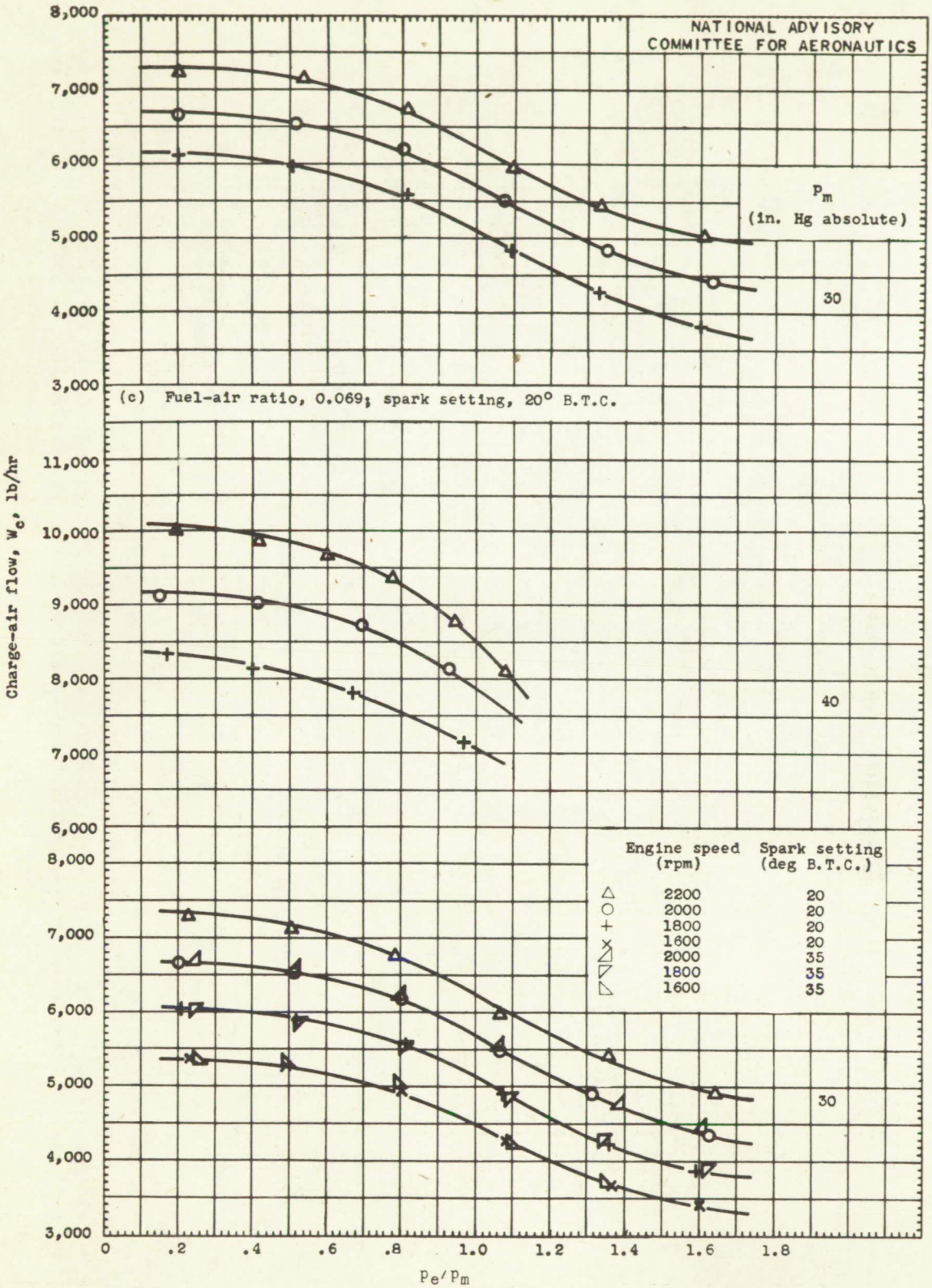

(d) Fuel-air ratio, 0.063; spark settings of 20° and 35° B.T.C. as noted.

Figure 8. - Concluded. Variation of charge-air flow W_c with p_e/p_m. Charge-air flow corrected to constant carburetor-air temperature of 550° R.

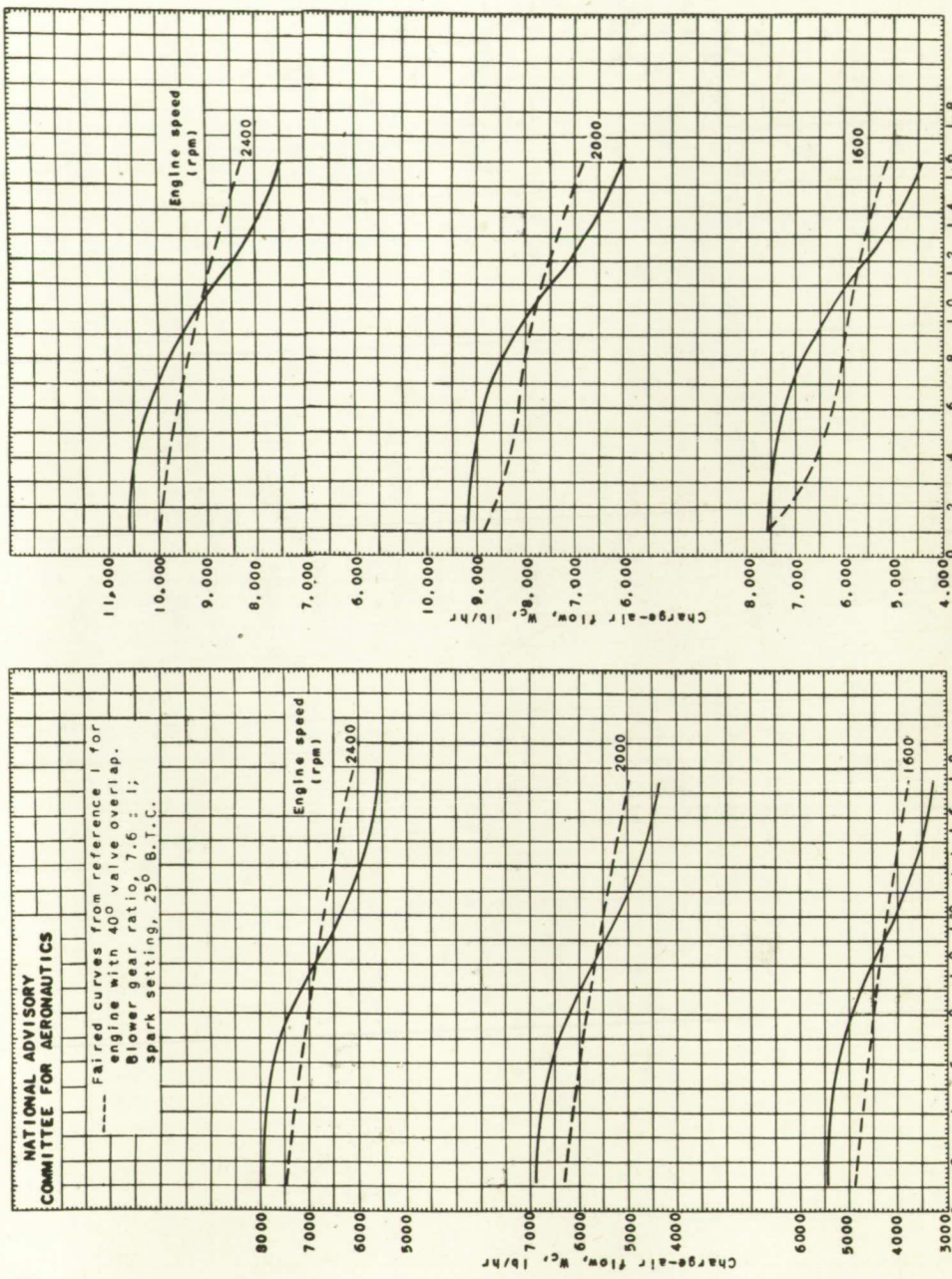

Figure 9. - Faired curves of charge-air flow W_c as taken from figure 8 plotted with faired curves of charge-air flow taken from reference 1. Charge-air flow corrected to constant carburetor-air temperature of 550° R; fuel-air ratio, 0.085.

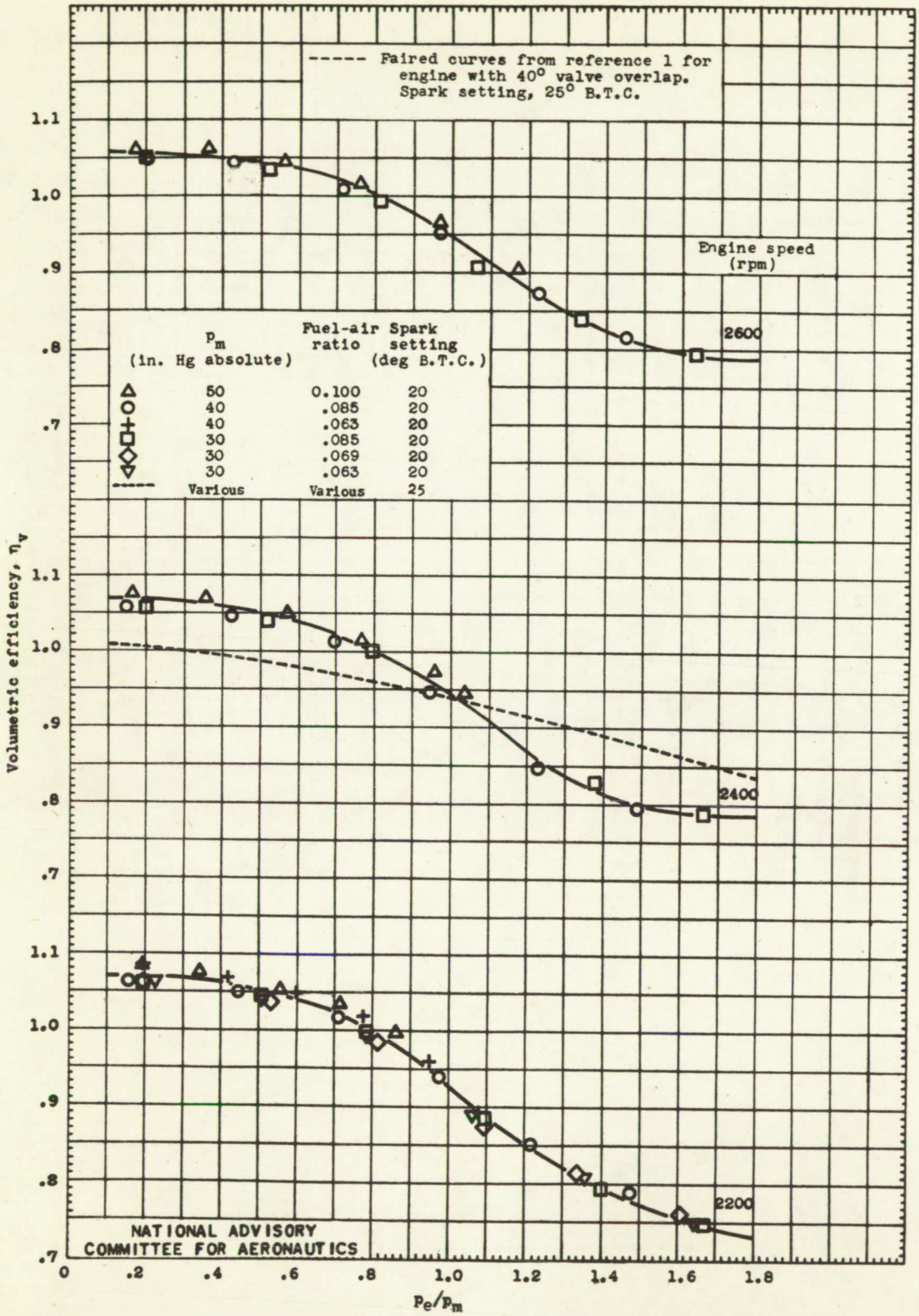

Figure 10.- Variation of volumetric efficiency η_v with p_e/p_m plotted with faired curves of volumetric efficiency taken from reference 1.

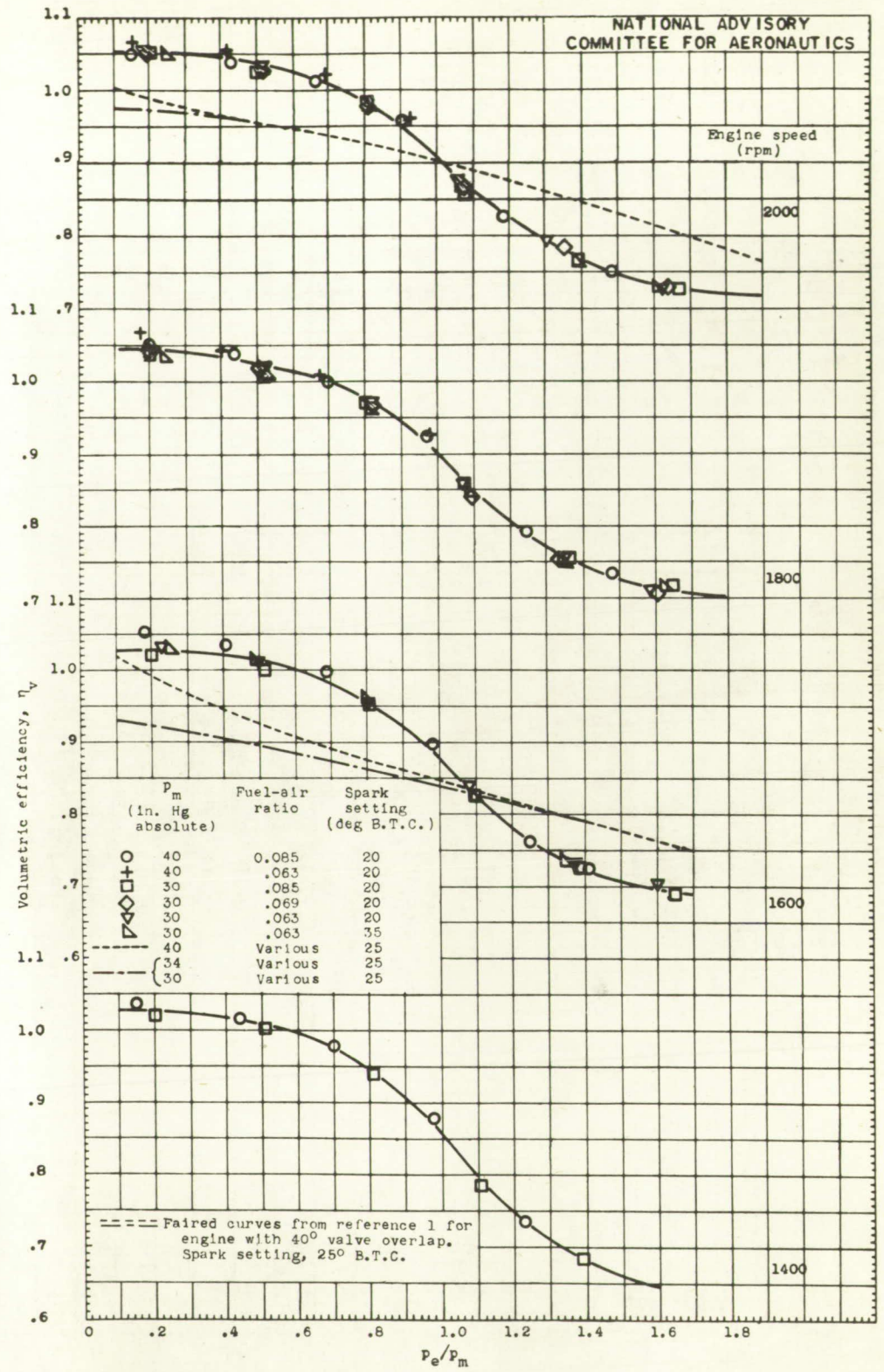

Figure 10. - Concluded. Variation of volumetric efficiency η_v with p_e/p_m plotted with faired curves of volumetric efficiency taken from reference 1.

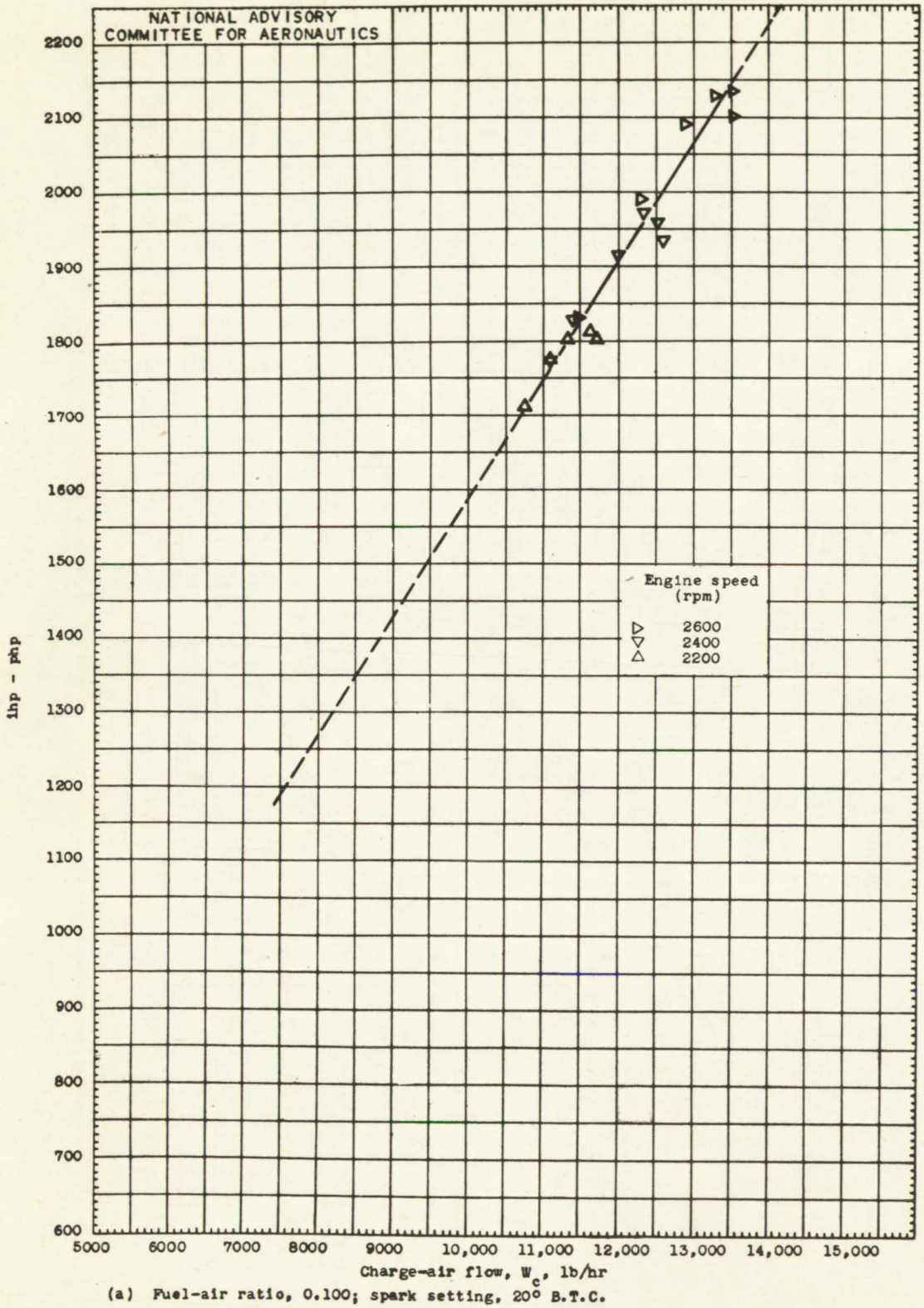

(a) Fuel-air ratio, 0.100; spark setting, 20° B.T.C.

Figure 11. - Variation of ihp - php with charge-air flow. ihp - php and W_c corrected to constant inlet-manifold temperature of 660° R.

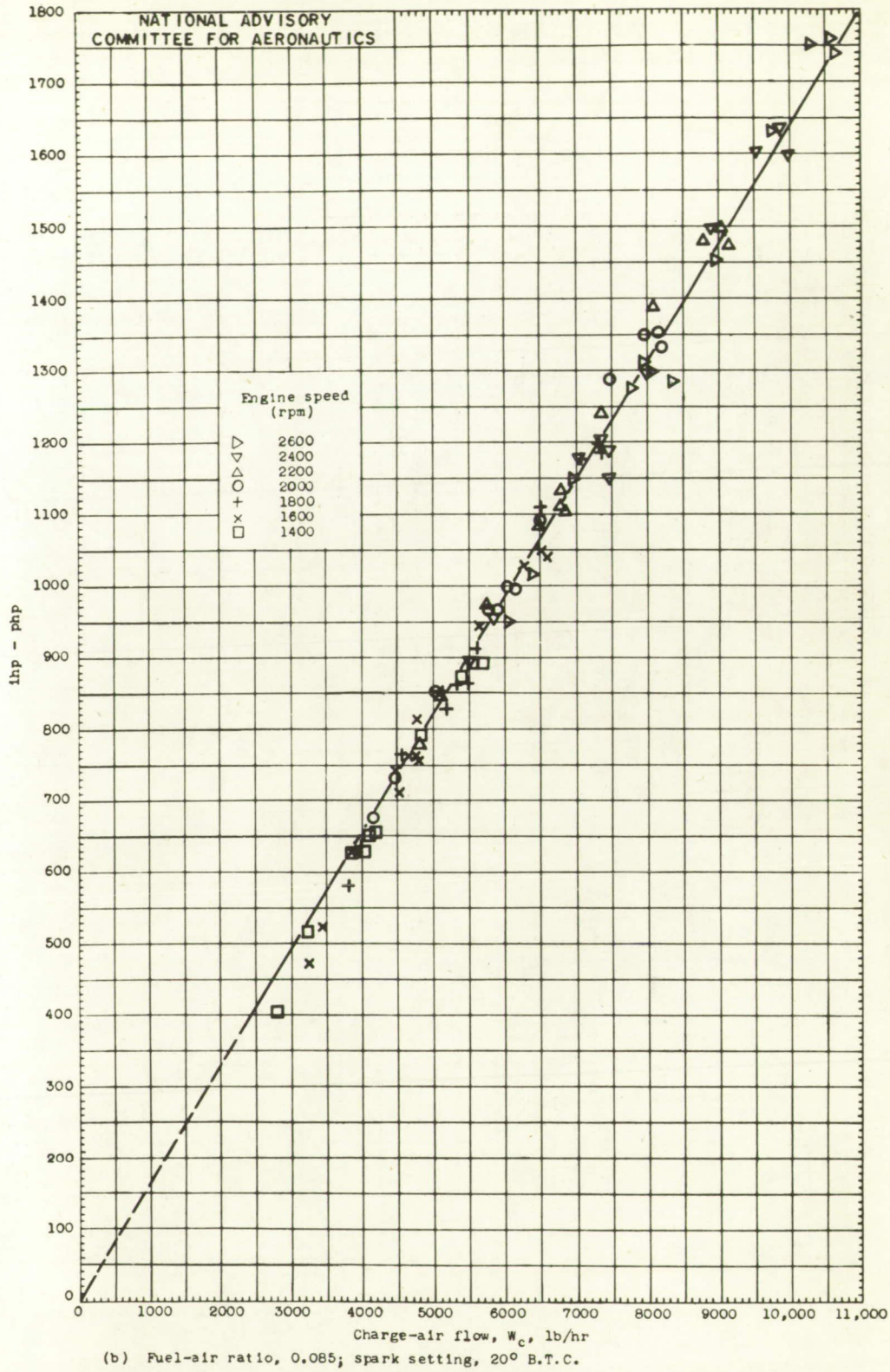

(b) Fuel-air ratio, 0.085; spark setting, 20° B.T.C.

Figure 11. - Continued. Variation of ihp - php with charge-air flow. ihp - php and W_c corrected to constant inlet-manifold temperature of 660° R.

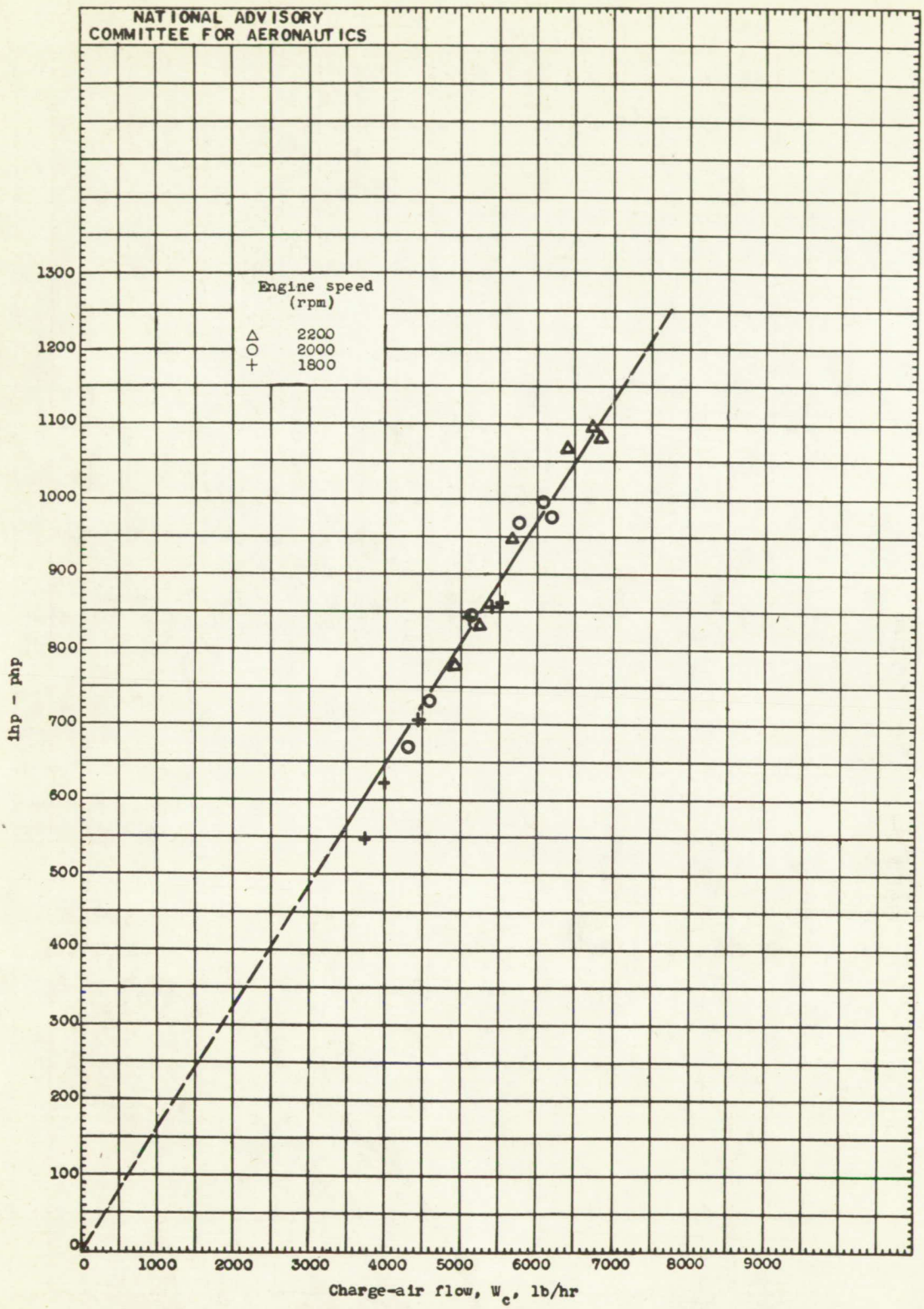

(c). Fuel-air ratio, 0.069; spark setting, 20° B.T.C.

Figure 11. - Continued. Variation of ihp - php with charge-air flow. ihp - php and W_c corrected to constant inlet-manifold temperature of 660° R.

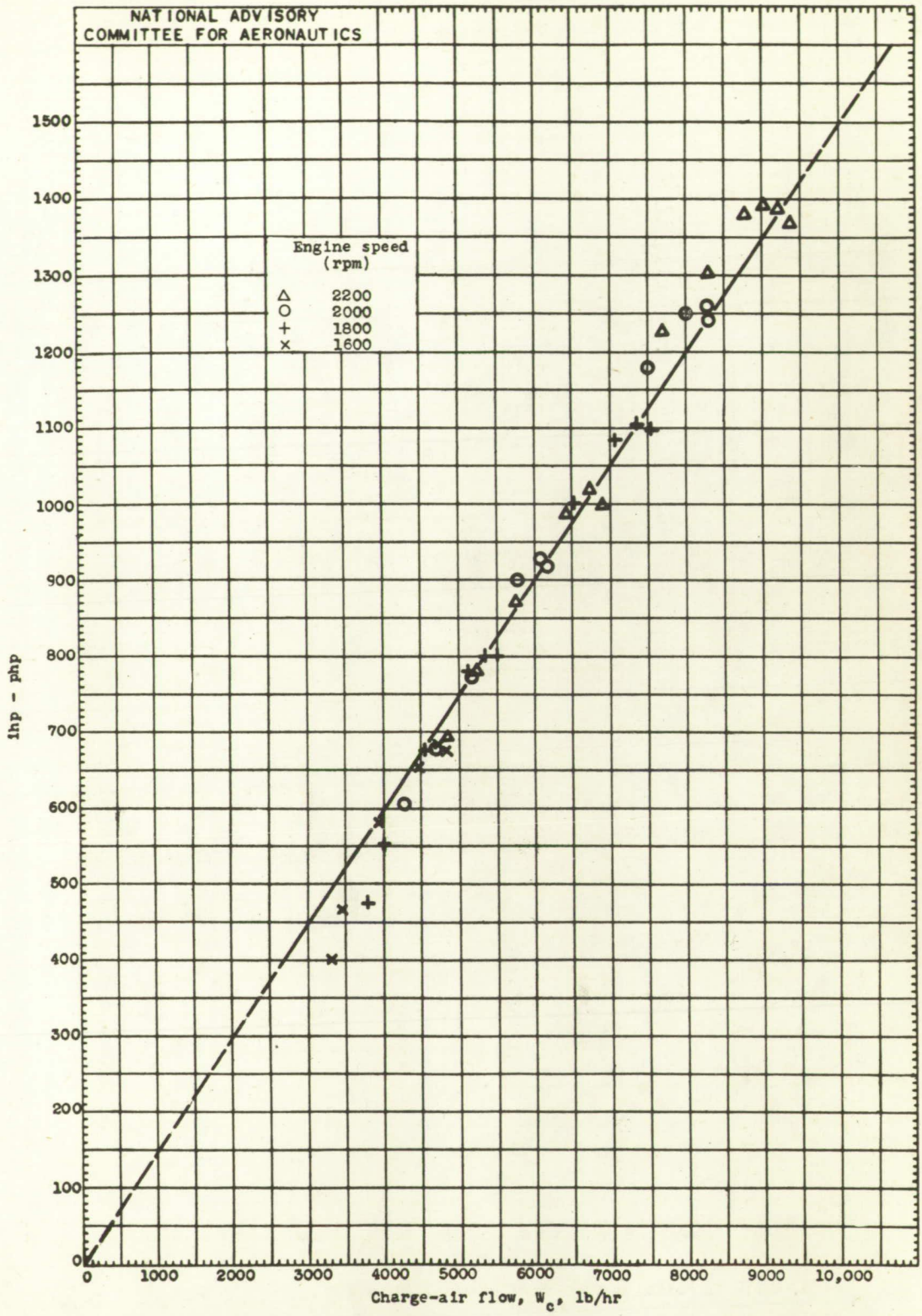

(d) Fuel-air ratio, 0.063; spark setting, 20° B.T.C.

Figure 11. - Continued. Variation of ihp - php with charge-air flow. ihp - php and W_c corrected to constant inlet-manifold temperature of 660° R.

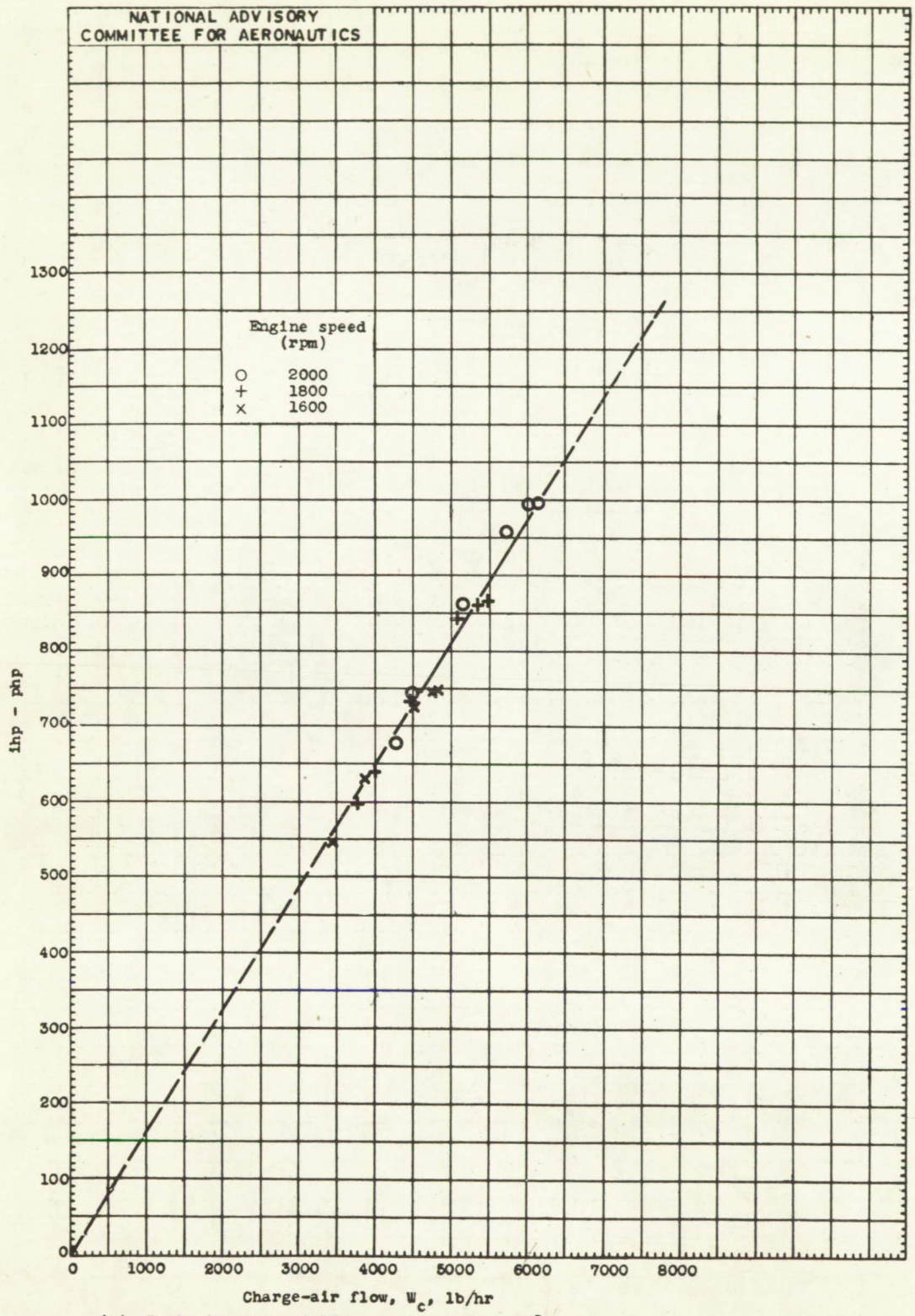

(e) Fuel-air ratio, 0.063; spark setting, 35° B.T.C.

Figure 11. - Concluded. Variation of ihp - bhp with charge-air flow. ihp - php and W_c corrected to constant inlet-manifold temperature of 660° R.

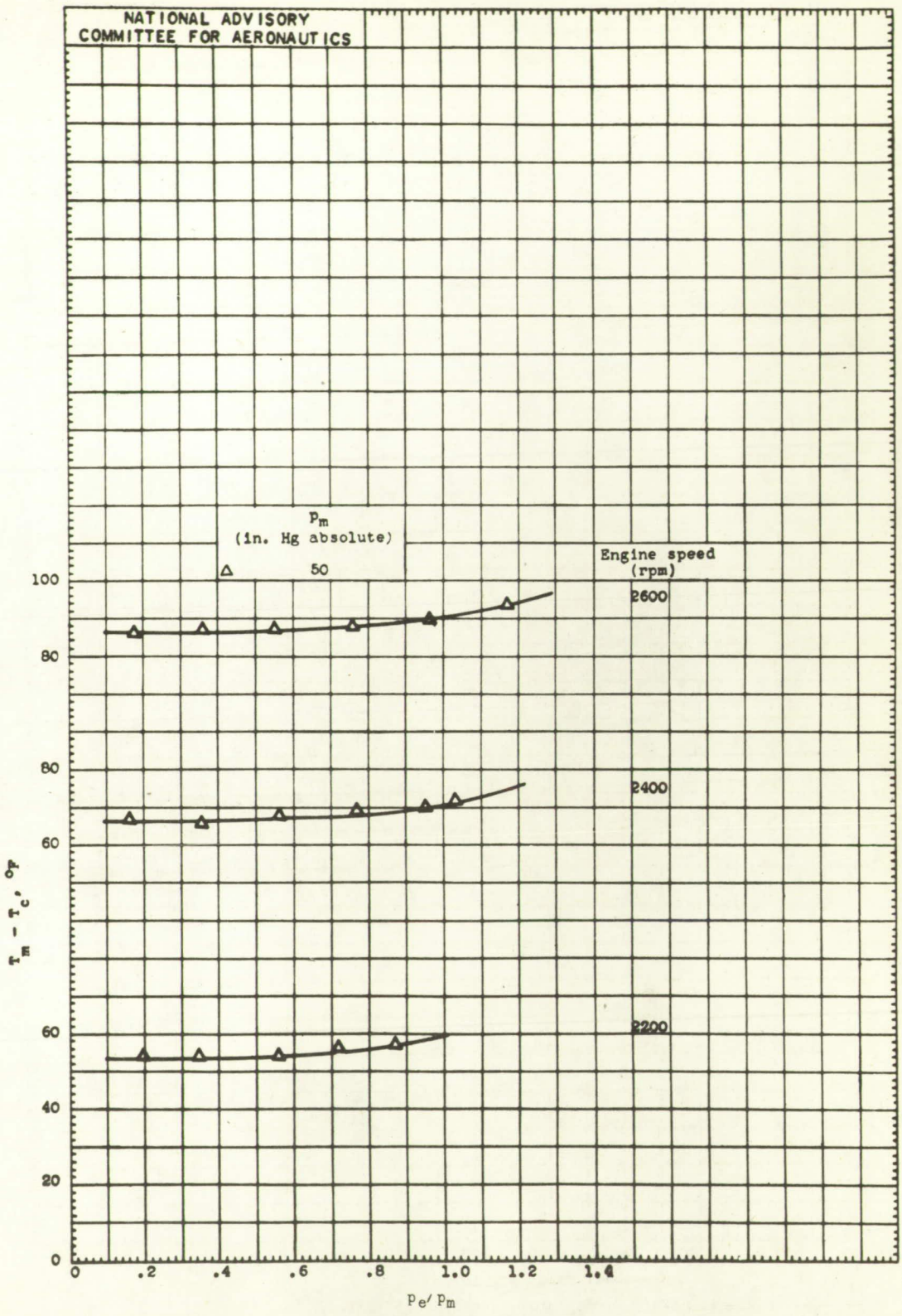

(a) Fuel-air ratio, 0.100; spark setting, 20° B.T.C.

Figure 12. - Variation of $T_m - T_c$ with p_e/p_m. Carburetor-air temperature T_c, approximately 550° R.

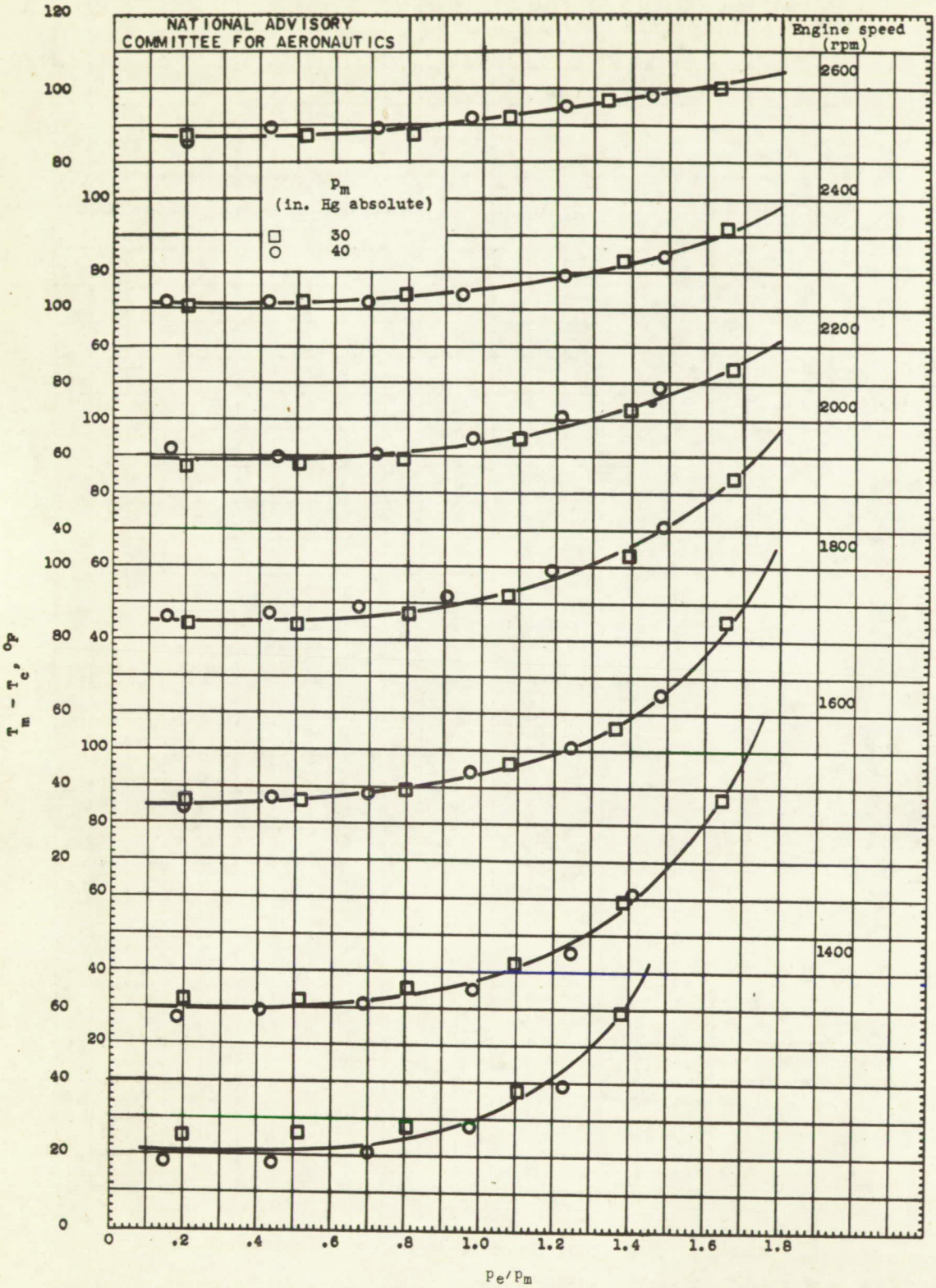

(b) Fuel-air ratio, 0.085; spark setting, 20° B.T.C.

Figure 12. - Continued. Variation of $T_m - T_c$ with p_e/p_m. Carburetor-air temperature T_c, approximately 550° R.

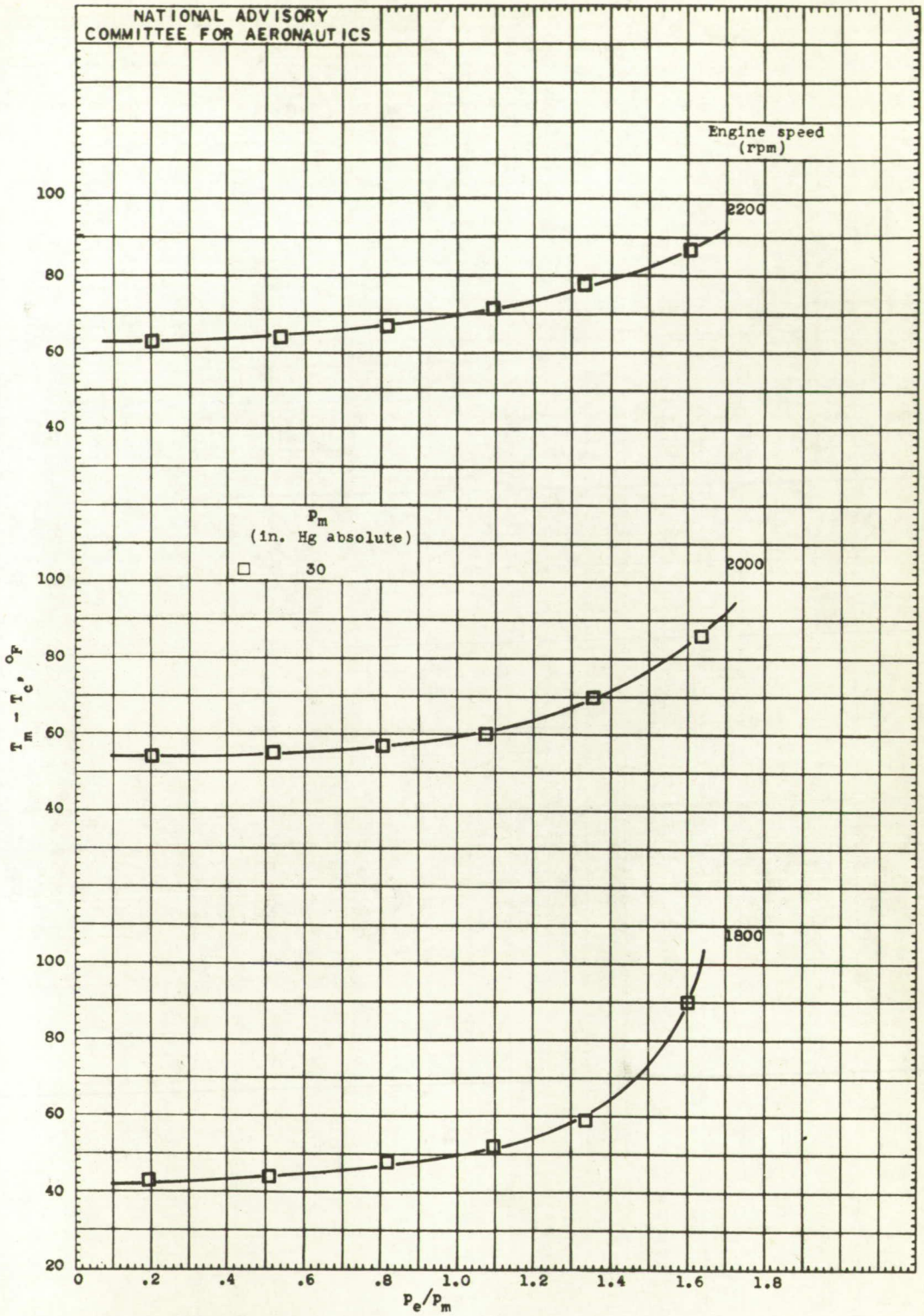

(c) Fuel-air ratio, 0.069; spark setting, 20° B.T.C.

Figure 12. - Continued. Variation of $T_m - T_c$ with p_e/p_m. Carburetor-air temperature T_c, approximately 550° R.

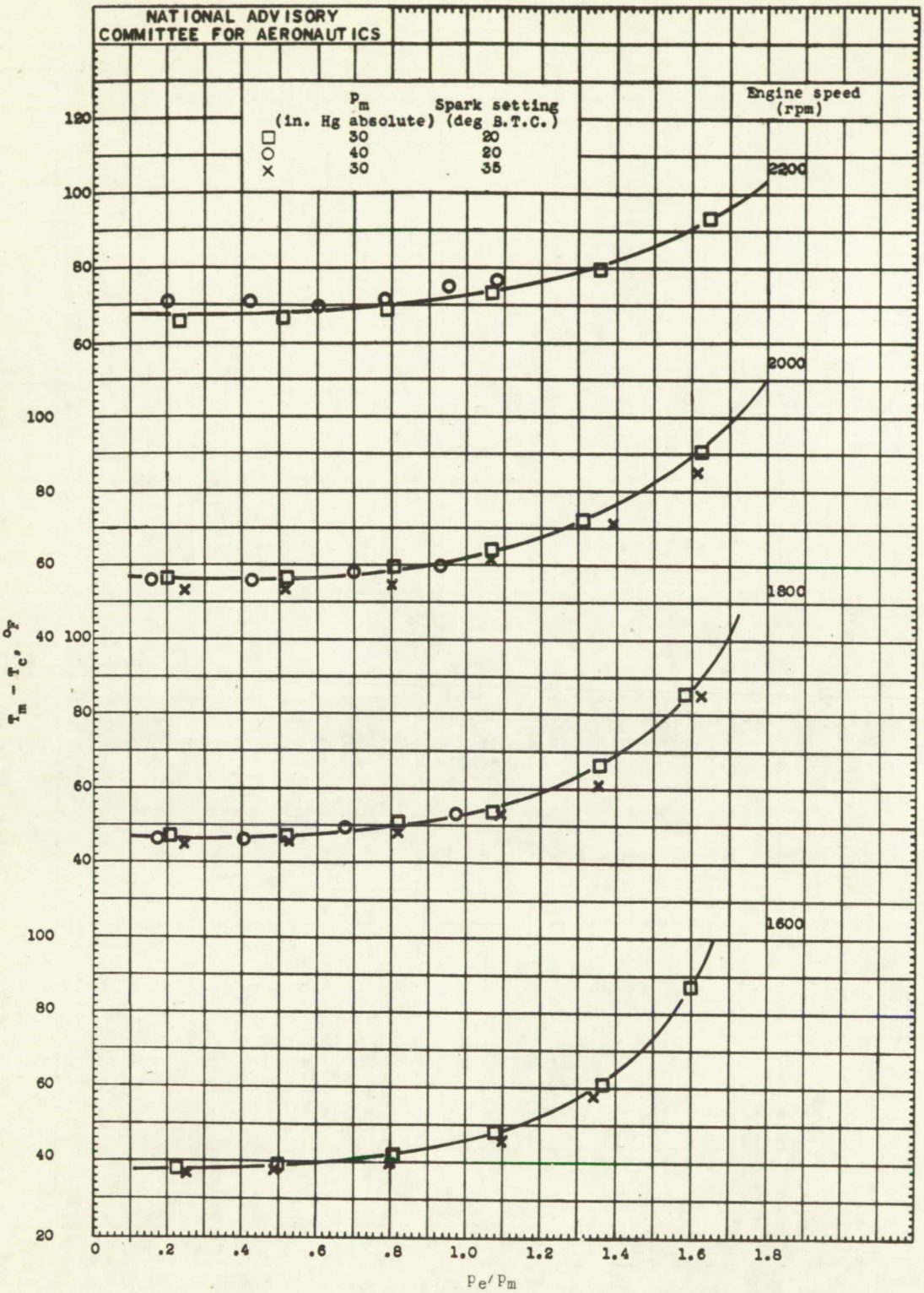

(d) Fuel-air ratio, 0.063; various spark settings.

Figure 12. - Concluded. Variation of $T_m - T_c$ with p_e/p_m. Carburetor-air temperature T_c, approximately 550° R.

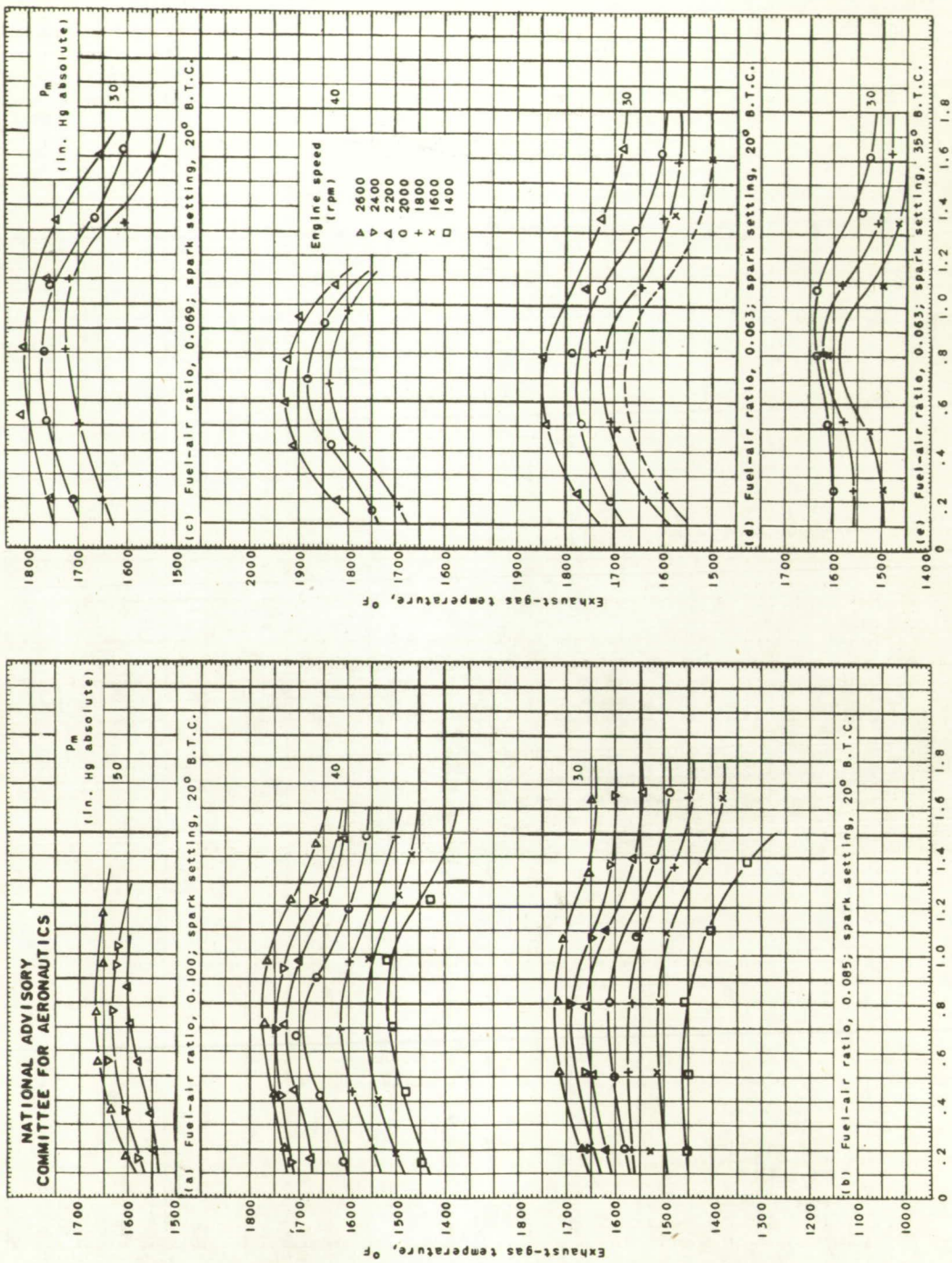

Figure 13. - Variation of exhaust-gas temperature with p_e/p_m for constant engine speeds, inlet-manifold pressures, and fuel-air ratios.

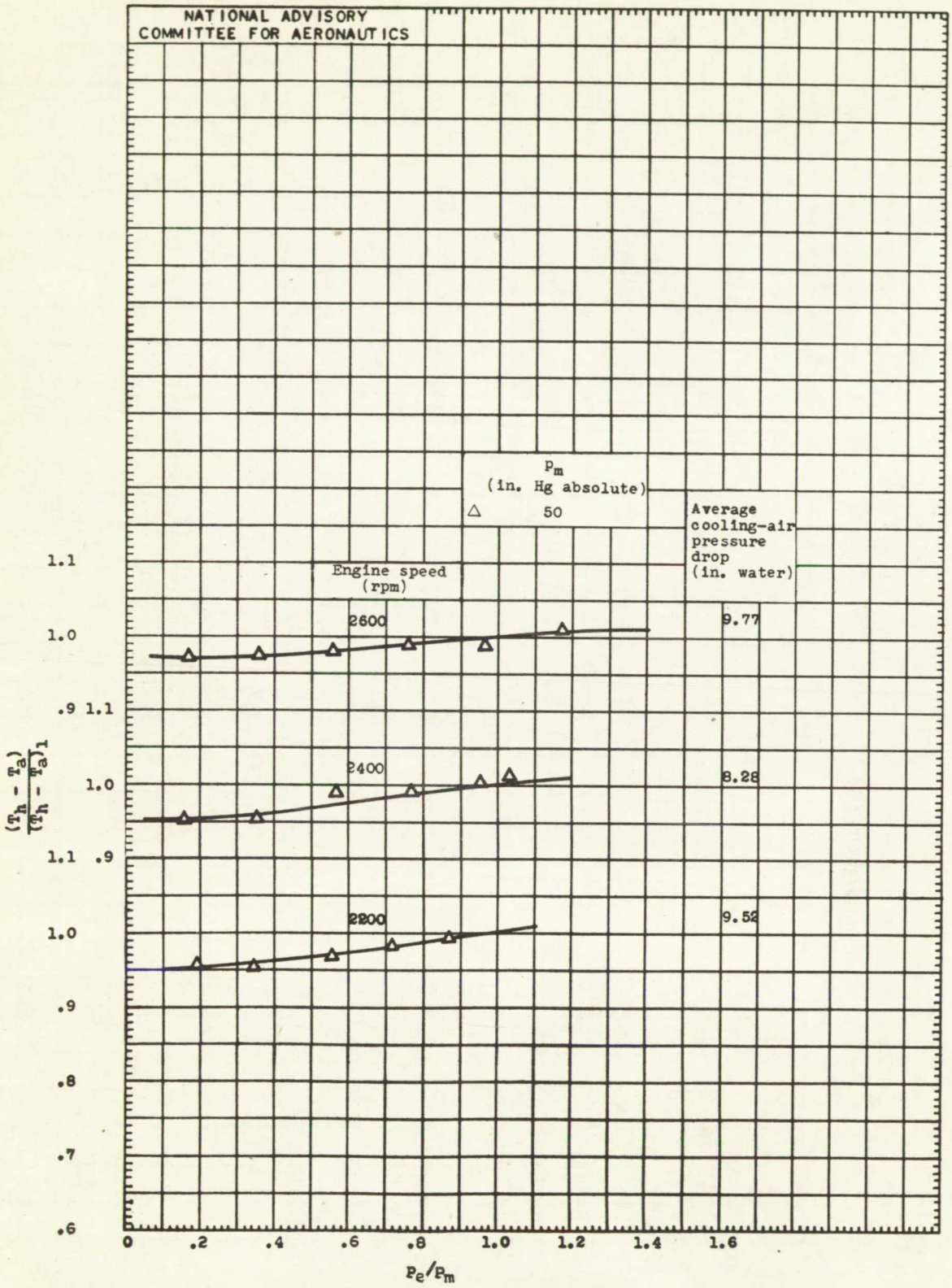

(a) Fuel-air ratio, 0.100; spark setting, 20° B.T.C.

Figure 14. - Variation of $(T_h - T_a)/(T_h - T_a)_1$ with p_e/p_m.

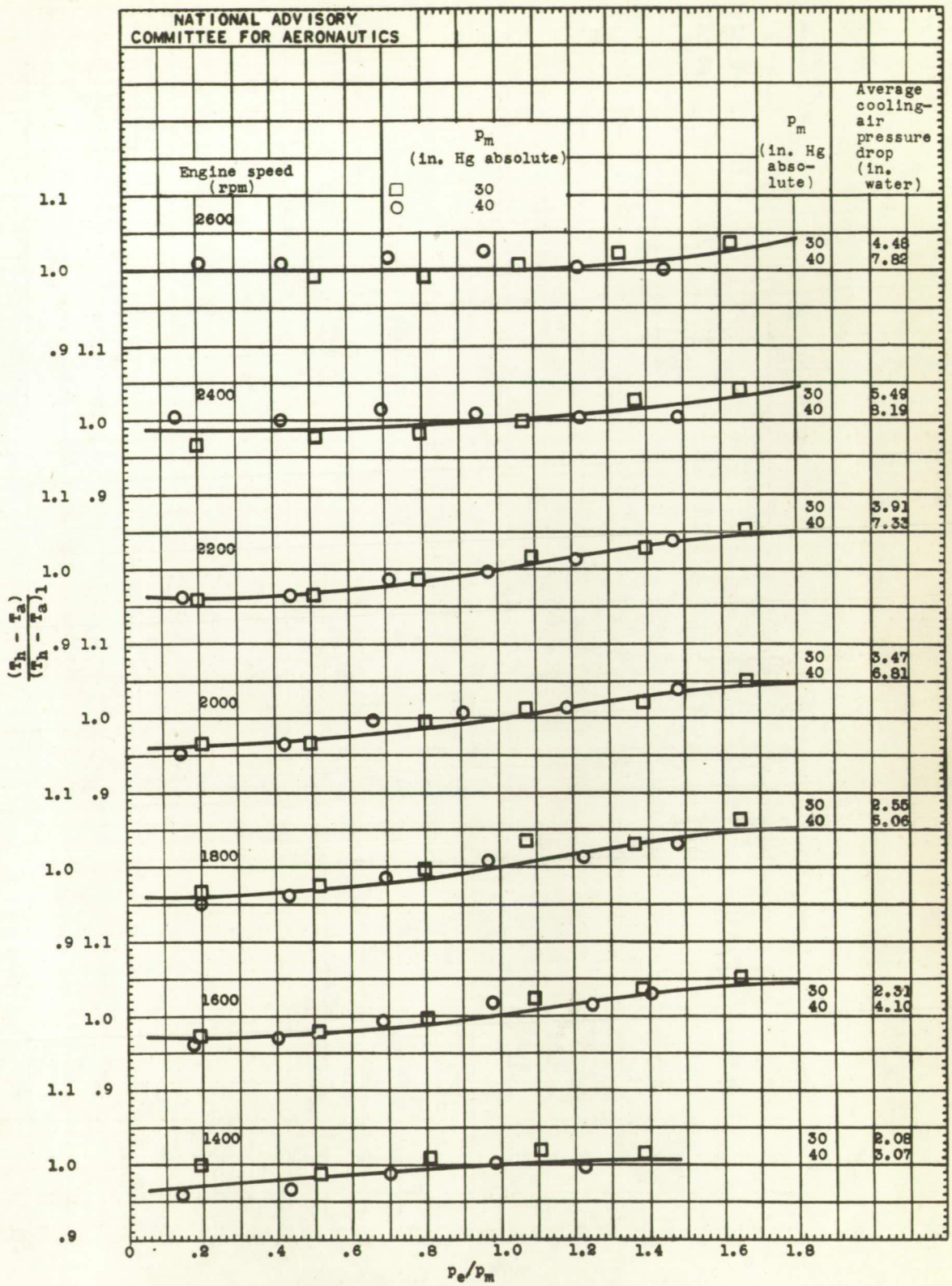

(b) Fuel-air ratio, 0.085; spark setting, 20° B.T.C.

Figure 14. - Continued. Variation of $(T_h - T_a)/(T_h - T_a)_1$ with p_e/p_m.

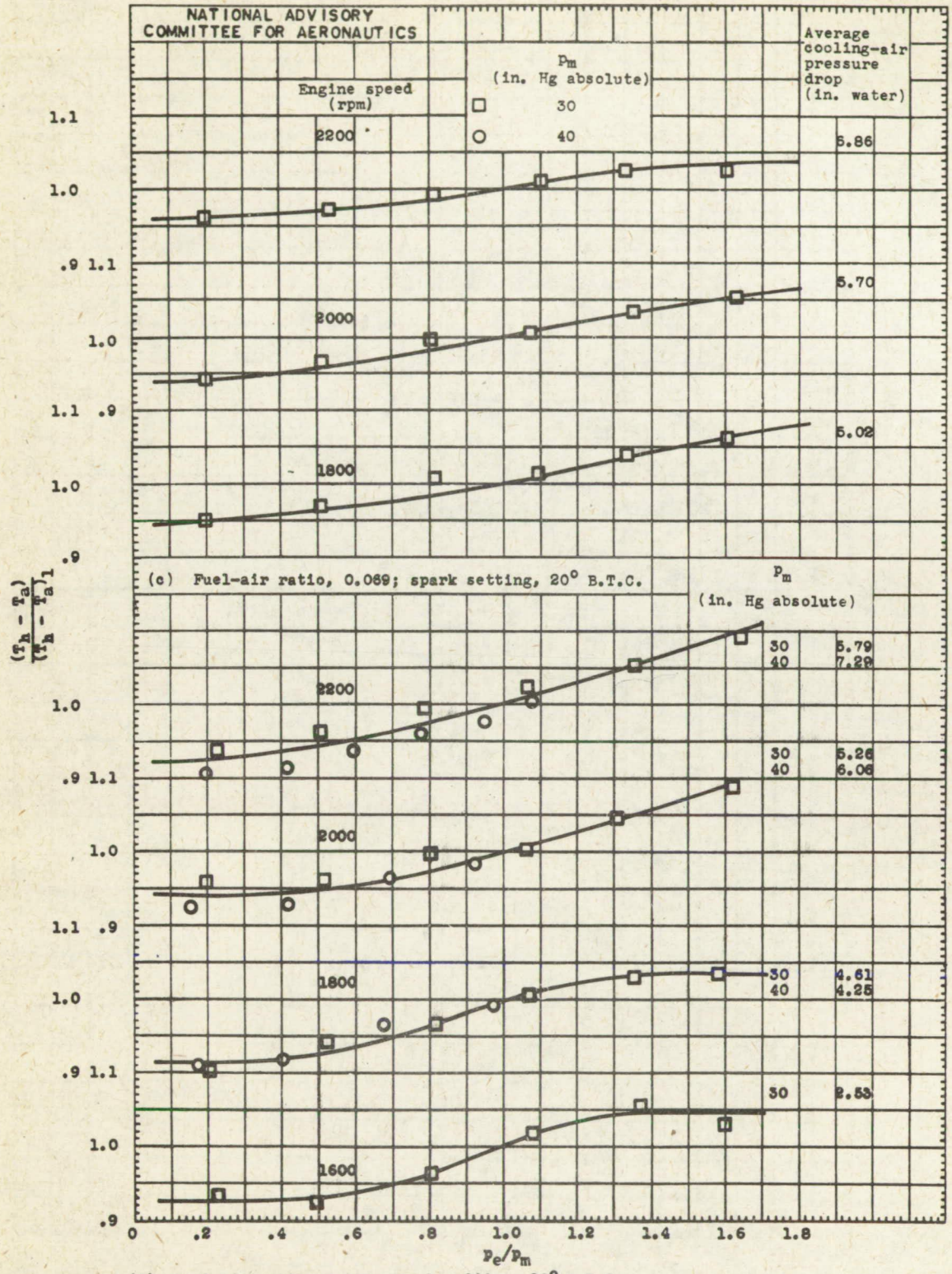

(d) Fuel-air ratio, 0.063; spark setting, 20° B.T.C.

Figure 14. - Continued. Variation of $(T_h - T_a)/(T_h - T_a)_1$ with p_e/p_m.

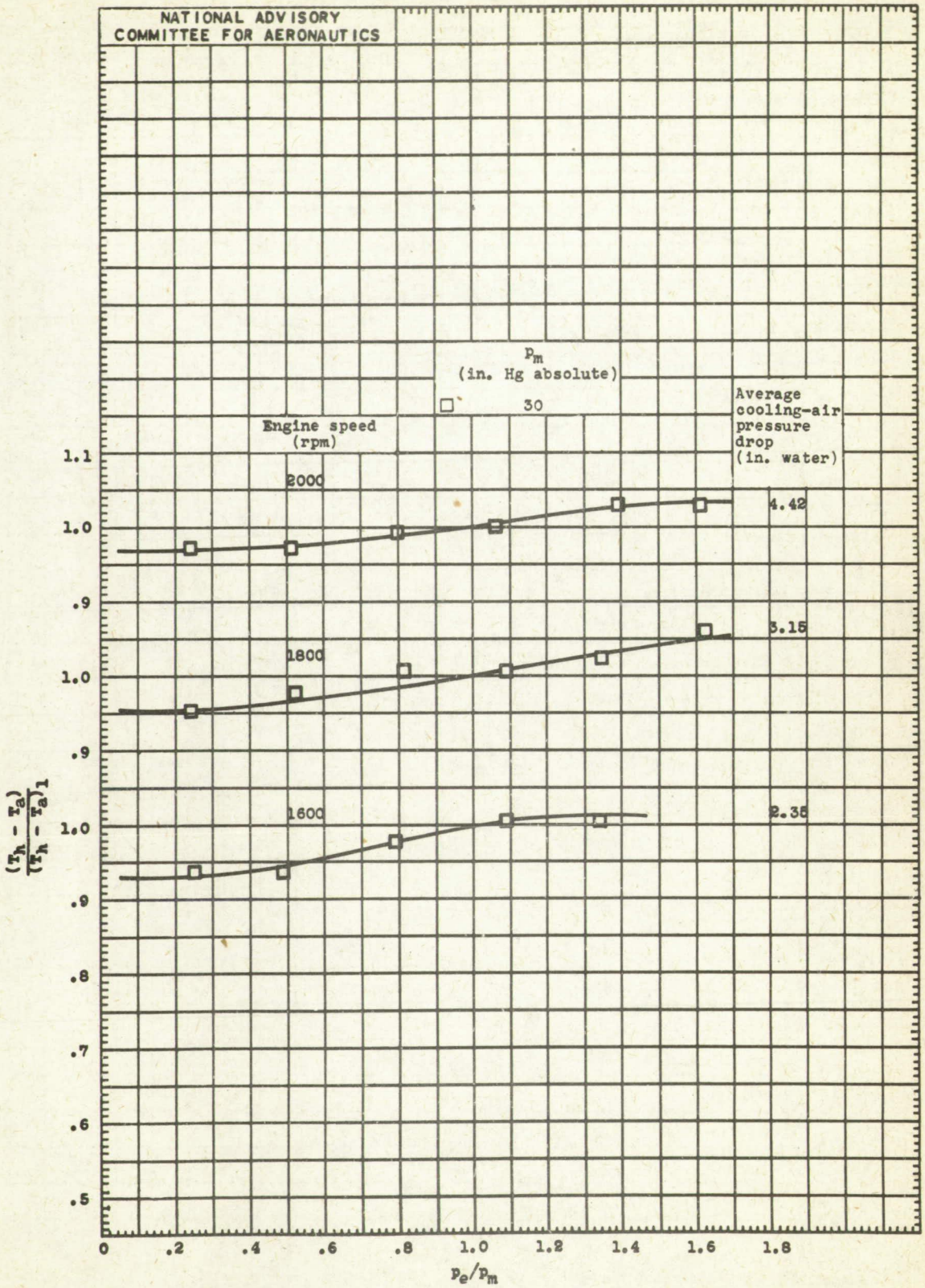

(e) Fuel-air ratio, 0.063; spark setting, 35° B.T.C.

Figure 14. - Concluded. Variation of $(T_h - T_a)/(T_h - T_a)_1$ with p_e/p_m.